Characterization of sympathetic preganglionic neuron activity during fictive locomotion in the *in vitro* neonatal mouse spinal cord

by

Chioma Victoria Nwachukwu

A thesis submitted to the Faculty of Graduate Studies of
The University of Manitoba
in partial fulfillment of the requirements of the degree of

MASTER OF SCIENCE

Department of Physiology and Pathophysiology
University of Manitoba
Winnipeg

Abstract

Spinal cord injury (SCI) is a life-altering neurological condition, with lost movement and impaired body functions caused by loss of communication between the brain and spinal cord (SC). Electrical stimulation of the lumbar SC has emerged as a powerful intervention for people with SCI. Clinical trials have shown its ability to improve both movements and lost autonomic body functions (e.g., blood pressure regulation, sweating, whole body metabolism). Although promising, neural mechanisms mediating observed recoveries using this intervention remain unknown, thus limiting its use for the wider SCI population. We hypothesized that ascending neurons from the lumbar SC provide direct synaptic input onto thoracic sympathetic preganglionic neurons (SPN) that, in turn, give homeostatic support to locomotion and exercise. Our lab recently showed that lumbar locomotor-related neurons synapse on SPNs throughout the thoracic SC. Thus, this study aims to characterize activity patterns of SPNs before and during fictive locomotion in the *in vitro* neonatal mouse SC. We pre-loaded fluorescent calcium dye into thoracic SPNs in the intermediolateral nucleus by applying reconstituted dye crystals to cut ends of thoracic ventral roots (VR). Using a high-speed camera, we recorded fluorescent signals emitted from labeled SPNs at baseline (non-locomotor) and during drug-induced fictive tonic and rhythmic VR activity. SPN calcium signals were then expressed as a change in fluorescence relative to baseline fluorescence intensity in labeled neurons. Our results indicate SPNs demonstrate rhythmic oscillations at baseline, which increase in amplitude during rhythmic VR activity. A higher proportion of SPNs in the T1-T7 segments show increased calcium fluorescence from baseline during tonic and rhythmic VR activity. In contrast, more SPNs in the T8-T13 segments demonstrate decreased fluorescence from their baseline. Fluorescence intensity changes <3% were considered insignificant. Finally, additional distinct SPNs become active with the appearance of tonic discharge or rhythmic locomotor activity. Together, these findings suggest there may be differences in SPN activity patterns at different rostrocaudal thoracic levels during VR locomotor activity. In the future, the results of this study may have practical implications for enhancing the efficacy of techniques like epidural stimulation to promote motor and specific autonomic recovery in people with SCI.

Acknowledgments

I want to express my sincere gratitude to my supervisors, **Drs. Jeremy Chopek** and **Kristine Cowley** for accepting me as their student. Jeremy, I still vividly remember the day I received your email acknowledging my interest in spinal cord research and inviting me for an interview. I was so excited; I could hardly sit still at work. Your belief in my potential encouraged me to strive for excellence throughout my studies. Kris, I remember my first chat with you over Zoom. Our conversation had me grinning from ear to ear for the rest of that day. I feel very fortunate to have learned from your wealth of knowledge and experience. I truly appreciate your patience, guidance, encouragement, and support throughout my stay. You constantly refined my ideas, troubleshot problems, and shared jokes even when the experiment was not going as planned. You have not only shared your expertise with me but also your friendship. Both of you contributed to an unforgettable experience I will always be grateful for. I would also like to thank my committee members, **Drs. Katinka Stecina** and **Brent Fedirchuk**. Katinka, your kindness on my first day at SCRC made me feel welcomed and left a lasting impression. I appreciate your support, teachings, and of course, cakes. Brent, I genuinely appreciate your invaluable feedback whenever I presented my work. Thanks to my lab members, **Lucia, Camila, Muniza,** and **Mary,** for their support and friendship. Thanks, **Juanita,** and **Sam,** for helping with my data analysis and figures. Thank you, **Shannon**, for relentlessly teaching me how to calculate those drug concentrations. My heartfelt thanks to **Matt and Narjes**. Indeed, I am grateful to the entire **SCRC** and all sponsoring agencies that have contributed to my growth as a scientist.

To my loving parents and sweet siblings, **Ije, Ezy, Chu, Amy**, and **Chidi**, I love you all. We are large, but I am yet to see a more tightly-knit family. Thanks for being my biggest cheerleaders. Thanks to all my other relatives for their never-ending support and prayers. Their belief in my abilities has been a source of strength and inspiration. I could not have achieved all I have today without their love, encouragement, and tireless efforts.

My deepest gratitude goes to my kids, **Som** and **Bube,** for their patience and for always cheering me on. Those short, sweet notes you sneaked under my pillow or bag kept me going daily. Thank you for putting up with my long hours of studying and occasionally missing out on fun events with understanding. Thank you to the love of my life, **ND** for his constant optimism and belief in me. We have been through thick and thin together, and I am truly grateful for your unending love and sacrifices. I feel so blessed to have you in my life.

To my friends, **Attiyeh, Berkan**, and **Samuel**, thanks for the support and laughter we shared throughout this journey. To my long-time friends, **Ifeoma and Chinonye**, and my precious gift, **Mama Mimi**, thanks for offering a shoulder to lean on in challenging times and celebrating my successes. We may be miles apart, but I do not take your love for granted.

To my co-workers at the **Department of Physiology, University of Nigeria**, I am grateful for your contribution towards my success as a graduate student. I am incredibly thankful to **Prof. Bond Anyaehie, Prof. Uche Nwagha, Prof. Ikenna Onwuekwe,** and **Dr. Ifeoma Orizu** for supporting my dreams.

To crown it all, I am eternally grateful to **God** for being so gracious to me and my family. Without God, I could not have accomplished this feat or made it this far. **Thank you, Jesus!**

Dedication

I dedicate this thesis to my loving family, who have been my biggest support system throughout this journey.

Table of Contents

List of Tables

List of Figures

List of Abbreviations

5HT (serotonin)

ANS (autonomic nervous system)

CGDA (calcium green conjugated dextran amine)

CnF (cuneiform nucleus)

CPG (central pattern generator)

CV (cardiovascular)

DA (dopamine)

DHK (dihydrokainic acid)

EPSP (excitatory postsynaptic potential)

ES (electrical stimulation)

GABA (gamma-aminobutyric acid)

IML (intermediolateral column)

IPSP (inhibitory postsynaptic potential)

MLR (mesencephalic locomotor region)

MN (motoneuron)

NE (norepinephrine)

NMDA (n-methyl-d-aspartate)

PNS (parasympathetic nervous system)

PPN (pedunculopontine nucleus)

PRV (pseudorabies virus)

PSN (propriospinal neurons)

raCSF (ringer's artificial cerebrospinal fluid)

RF (reticular formation)

ROI (regions of interest)

RVLM (rostral ventrolateral medulla)

RVMM (rostral ventromedial medulla)

SC (spinal cord)

SCI (spinal cord injury)

SNS (sympathetic nervous system)

SPN (sympathetic preganglionic neuron)

TMR (tetramethylrhodamine)

TTL (transistor-transistor logic)

TTX (tetrodotoxin)

VH (ventral horn)

VR (ventral root)

Chapter I: Introduction

1.1 Overview of Spinal Cord Injury

Spinal cord injury (SCI) is a life-altering neurological event, with lost movement and impaired multiple organ functions caused by loss of communication between the brain and spinal cord (SC). SCI not only has the potential to affect the physical well-being of an individual but also negatively impacts their mental and social welfare (Singh, Tetreault et al. 2014). In addition to decades of living with permanent disability owing to injury (McDonald and Sadowsky 2002, Anderson 2004), the long-term treatment cost of people with SCI constitutes a substantial economic burden on the individuals, their families, and society (Noonan, Fingas et al. 2012). People with SCI can suffer significant motor and sensory impairments depending on the level and severity of the injury. The American Spinal Injury Association Impairment Scale (AIS) is a standardized neurological classification scale for SCI used to assess a person's functional disability following injury (Roberts, Leonard et al. 2017). In this system, AIS classifies SCI as complete or incomplete, with the former designated as Grade A and the latter on a continuum with Grades B through E (**Table 1**). By definition, a complete SCI refers to the total loss of all sensory and motor functions below the level of injury, including the lowest sacral segments (Roberts, Leonard et al. 2017). On the other hand, incomplete injuries are those with some preserved sensory or motor function below the level of injury (Roberts, Leonard et al. 2017). More recently, injuries have also begun to be classified as autonomically complete or incomplete, but this is an emerging area in the clinical SCI realm (Wecht, Krassioukov et al. 2021).

A	Complete; no motor or sensory function is preserved in the sacral segments S4–S5.
B	Incomplete; sensory function is preserved, but not motor function is preserved below the neurological level and includes the sacral segments S4–S5.
C	Incomplete; motor function is preserved below the neurological level, and more than half of key muscles below the neurological level have a muscle grade of less than 3.
D	Incomplete; motor function is preserved below the neurological level, and at least half of key muscles below the neurological level have a muscle grade of 3 or more.
E	E Normal; motor and sensory function are normal.

Table 1: American Spinal Injury Association Impairment Scale

There are multiple ways to sustain injury to the spinal cord. SCI can occur following trauma such as motor vehicle/ motorcycle crashes, falls, assault/violence, sports-related accidents, or non-traumatic causes like infections, tumors, vascular disorders, developmental and degenerative conditions, and iatrogenic causes, among others (Noonan, Kwon et al. 2012, Chen, Tang et al. 2013, Müller-Jensen, Ploner et al. 2021) . Historically, up to 90% of reported injuries are due to traumatic causes (World Health Organization 2013), with automobile crashes and falls being the most common causes of injury (Noonan, Fingas et al. 2012, Chen, Tang et al. 2013, World Health Organization 2013). Although there is no reliable data on the global prevalence of these injuries, WHO reported that between 250,000 and 500,000 people worldwide sustain varying levels of spinal cord injury yearly (WHO 2013). Of these new injuries, traumatic SCI is estimated at 179,312 cases per year globally (Lee, Cripps et al. 2014). In North America alone, ~12,500 new cases of SCI are recorded annually (Hachem, Ahuja et al. 2017). Over 85,000 Canadians presently live with the effects of SCI, with a higher incidence seen in males than females (Noonan, Fingas et al. 2012).

SCI is an event that can affect people of all ages. Although the mechanisms of injury vary, some mechanisms are more frequent in specific age groups. The mean age for Canadians whose injuries were secondary to a fall was reported as 61 years, while those whose injuries were sport or transport-related were, on average, 41 and 43 years old, respectively (Noonan, Fingas et al. 2012, Singh, Tetreault et al. 2014). Damage to the spinal cord can occur at any segmental level. The most common injury site is the cervical spine, and most injuries are of the incomplete type (Kang, Ding et al. 2018). Motor impairments following SCI differ according to the level and severity of the injury. Regarding motor paralysis, tetraplegia has been reported to be more commonly seen than paraplegia in all spinal cord injuries across most countries except Canada and Turkey (Kang, Ding et al. 2018). However, a higher prevalence of tetraplegia has also been documented in Canadians with traumatic SCI (Noonan, Fingas et al. 2012).

The global economic burden associated with SCI is substantial. The lifetime economic costs of SCI in Canada are estimated to range from $1.5 million for an individual with incomplete paraplegia to $3.0 million for one with complete tetraplegia. The annual economic burden for Canadians with traumatic SCI is approximately $2.67 billion (Noonan, Kwon et al. 2012, Krueger, Noonan et al. 2013). This economic burden addresses both indirect ($1.10 billion) and direct ($1.57 billion) costs (Krueger, Noonan et al. 2013). Due to the variety of secondary complications that frequently accompany SCI, spinal cord-injured individuals have a substantially lower average life expectancy than their peers without SCI (Noonan, Fingas et al. 2012, Krueger, Noonan et al. 2013). As published by the 2009 National Spinal Cord Injury Statistical Center (NSCISC) report, life expectancy for an individual with SCI depends on the level and severity of the injury, age at injury, residual neurologic function, and ventilator dependency. According to the WHO, people with SCI are 2 to 5 times more likely to die

prematurely than those without injury (WHO, 2013). The global mortality rate ranges from 3.1% to 22.2% in developed countries and 1.4% to 20.0% in non-developed countries (Kang, Ding et al. 2018).

1.1.1 Secondary Complications of Spinal Cord Injury

Besides the physical disability associated with damage to the spinal cord, people with spinal cord injuries frequently suffer secondary complications. More than 95% of spinal cord-injured individuals report at least one secondary health condition, and over half report three or more (Anson and Shepherd 1996). Some of these secondary complications begin in the acute phase of the injury, while most others are longer-term health problems. Chronic complications especially interfere with one's independence and overall quality of life. These range from spasticity and chronic pain (Rekand, Hagen et al. 2012, Rekand, Hagen et al. 2012, Finnerup 2017) to sedentary-related diseases like obesity (Crane, Little et al. 2011, Wen, Chen et al. 2018), glucose intolerance or diabetes (Duckworth, Solomon et al. 1980, Duckworth, Jallepalli et al. 1983). SCI can also result in a variety of respiratory problems (Berlowitz, Wadsworth et al. 2016), bowel and bladder irregularities (Stiens, Bergman et al. 1997, Potter 2006), sexual issues (Sipski 1991), osteoporosis and bone fracture (Garland, Stewart et al. 1992, Frotzler, Cheikh-Sarraf et al. 2015, Peppler, Kim et al. 2017), depression (Williams and Murray 2015), infections (Garcia-Arguello, O'Horo et al. 2017, Jaja, Jiang et al. 2019), thermoregulatory and cardiovascular (CV) dysfunction (Myers, Lee et al. 2007, Weaver, Fleming et al. 2012, Eldahan and Rabchevsky 2018, Mneimneh, Moussalem et al. 2019). The presence of secondary complications is a crucial determinant of mortality following SCI (WHO, 2013).

Historically, renal and respiratory complications were considered the most common causes of death for people with SCI (Furlan and Fehlings 2008). However, in recent years, cardiovascular dysfunction is exceedingly a concerning secondary complication of SCI (reviewed in Myers, Lee et al. 2007). It is now recognized as the leading cause of mortality in acute and chronic injuries, often presenting as orthostatic hypotension, autonomic dysreflexia, heart rate abnormalities, and impaired cardiovascular reflexes (Garshick, Kelley et al. 2005, Furlan and Fehlings 2008, Hagen, Faerestrand et al. 2011, Hagen, Rekand et al. 2012). It has been established that cardiovascular risk factors and diseases are more prevalent in people with SCI compared to ambulatory non-disabled persons. This heightened risk of CV dysfunction is not only due to the loss of descending pathways mediating CV response but also likely due to the inability of SCI persons to engage in locomotor activity and whole-body exercise (Myers, Lee et al. 2007, Cowley 2018).

1.2 Anatomy and Neural Pathways Controlling Locomotion

Locomotion is one of the most basic motor tasks of animals and humans. In neurologically intact animals, locomotion is initiated by descending input from supraspinal regions (cortex, brainstem). Although locomotion seems like a simple task, it is, in reality, a complex motor behavior involving a variety of neural networks in the brain and the spinal cord. The neural structures involved in the control of movements of the body and posture in vertebrates, including humans, can generally be organized into four complementary subsystems, namely, the brainstem and spinal cord circuits, descending modulatory pathways, the cerebellum, and basal ganglia (Purves et al. 2001). These distinct but complementary neuronal groups or

projections ensure that voluntary and involuntary motor commands are initiated and executed as required.

1.2.1 Brainstem Neural Circuits for Locomotion:

In neurologically intact animals, the brain and spinal locomotor neuronal circuits work together to initiate and modulate locomotion, and several reviews have attempted to address the complexity of these systems (Grillner 1975, Armstrong 1986, Mori 1987, Jordan 1991, Whelan 1996). Electrophysiological and anatomical neurophysiology research led to discoveries of supraspinal structures, namely the mesencephalic locomotor region (MLR) and the medullary reticular formation (RF), playing critical roles in initiating and modulating locomotion. The MLR, when stimulated, was demonstrated to activate directly or indirectly reticulospinal neurons, which in turn activate spinal locomotor central pattern generators that in turn activate motoneurons to induce stepping (Shik, Severin et al. 1969, McClellan and Grillner 1984, Garcia-Rill and Skinner 1987, Noga, Kriellaars et al. 1991, Perreault, Drew et al. 1993, Jordan 1998, Jordan, Liu et al. 2008). Stimulation studies (Drew and Rossignol 1984, Drew 1991, Liu and Jordan 2005, Szokol, Glover et al. 2011), as well as lesion studies (Steeves and Jordan 1980, Eidelberg 1981), have shown pontomedullary RF neurons to contribute to initiation and modulation of locomotor patterns of activity.

In vitro studies have also used trains of electrical stimulation applied to the brainstem to induce locomotor-like activity in neonatal rat brainstem–spinal cord preparation (Zaporozhets, Cowley et al. 2004, Liu and Jordan 2005, Cowley, Zaporozhets et al. 2008, Cowley, Zaporozhets et al. 2009, Cowley, Zaporozhets et al. 2010). Optogenetic experiments have also demonstrated

the role of different brainstem structures in promoting locomotor activity. Targeted light activation of glutamatergic neurons in MLR cuneiform (CnF) and pedunculopontine (PPN) nuclei led to the initiation of locomotion in previously resting animals (Caggiano, Leiras et al. 2018). In the study, slow explorative behaviors were thought to be mediated by the activity of CnF neurons, while fast escape behaviors were seen with PPN activation (Caggiano, Leiras et al. 2018). This is consistent with reports of accelerated and decelerated locomotor rhythms observed on photostimulating CnF and PPN neurons, respectively (Josset, Roussel et al. 2018). Interestingly, anatomically identified distinct subpopulations of MLR excitatory neurons have been demonstrated to be recruited in other behaviors (posture, handling, and grooming) besides locomotion (Ferreira-Pinto, Kanodia et al. 2021). The latter was observed explicitly in stimulating glutamatergic MLR neurons that project predominantly to the medulla (Ferreira-Pinto, Kanodia et al. 2021).

As much as these bulbospinal neuronal projections are necessary for locomotor behaviors, they are not considered essential since the spinal cord itself contains the neural circuitry sufficient to produce locomotion (Graham Brown 1911, Graham Brown 1914, Noga, Kriellaars et al. 1991, Cazalets, Borde et al. 1995, Brustein and Rossignol 1998).

1.2.2 Spinal Neural Circuits for Locomotion:

After spinal cord injury, there is impaired movement due to the loss of communication between the supraspinal structures and spinal cord neural circuits. Nonetheless, it has been established that the mammalian spinal cord has the intrinsic ability to generate rhythmic locomotor-like activity independent of descending command signals (Graham Brown 1911,

Grillner 1975, Delcomyn 1980). The capability to generate and coordinate mammalian locomotion is thought to be due to regionally distributed neural networks within the spinal cord tissue known as the locomotor "central pattern generators (CPG)" (Cowley and Schmidt 1997, Griener, Dyck et al. 2013, Kiehn 2016, Haque and Gosgnach 2019). The spinal locomotor system has been described to consist of two groups of neurons: rhythm-generating neurons and pattern-formation neurons (McCrea and Rybak 2008). While the former drives the rhythmic motor behavior, the latter coordinates movement on both sides of the body and provides for alternation between flexors and extensors within a limb (Rybak, Shevtsova et al. 2006, McCrea and Rybak 2008, Kiehn 2016). Early investigations into the functionality of spinal locomotor circuitry were done in cats (Shik, Severin et al. 1969, Stuart and Hultborn 2008). However, several other studies have described the presence and distribution of intrinsic spinal locomotor networks in various animal species (Grillner 1974, Cohen and Wallen 1980, Kahn and Roberts 1982, Ho and O'Donovan 1993, Cowley and Schmidt 1997).

It is now well established that locomotor CPGs exist in the spinal cord, with a concentration of coordinating populations of interneurons located in the cervical and lumbar spinal cord. These interneurons coordinate the activity of motoneurons that innervate the trunk and limbs muscles during overground locomotion (Viala and Vidal 1978, Cazalets, Borde et al. 1995, Kjaerulff and Kiehn 1996, Ballion, Morin et al. 2001, Rossignol and Frigon 2011, Frigon 2017). These CPG circuits receive multiple supraspinal, spinal, and afferent inputs (Marder and Bucher 2001, Rossignol and Frigon 2011) and can be activated in various ways, including direct neurotransmitter activation and via descending systems. Different monoamines are involved in the activation of components of the spinal locomotor network. Serotonin and its role in locomotion continue to be extensively investigated. Studies suggest that serotonin axon terminals

are distributed throughout all the spinal levels (Rajaofetra, Sandillon et al. 1989, Hornung 2003); and play a significant role in the modulation of spinal locomotor networks (Cazalets, Sqalli-Houssaini et al. 1992, Cowley and Schmidt 1994, Schmidt and Jordan 2000). Like serotonin (5HT), bath application of several other neurochemicals to *in vitro* preparations, including acetylcholine, noradrenaline, glutamate, NMDA (n-methyl-d-aspartate), DHK (dihydrokainic acid), and DA (dopamine), induces locomotor-like activity in decerebrate or spinalized animals (Barbeau and Rossignol 1991, Kiehn, Hultborn et al. 1992, Cowley and Schmidt 1994, Kiehn and Kjaerulff 1996, Cowley, Zaporozhets et al. 2005) It has been demonstrated that different neurochemicals applied alone or in combination activate distinct spinal rhythm-generating networks to produce locomotor-like and non-locomotor-like activity in the *in vitro* spinal cord preparation (Cowley and Schmidt 1997). However, stable fictive locomotion in the *in vitro* rodent preparations has been best achieved using a combination of at least 5HT and NMDA receptor agonists. Cazalets et al. (1992) suggested that serotonin acts directly on the oscillator component of the CPG to induce fictive locomotion. This was due to the observed dose-dependent increase in the ventral root (VR) bursts with bath application of 5HT to isolated rodent spinal preparation. Other work demonstrated that 5HT is required for NMDA to display membrane potential voltage oscillations, even in the absence of other synaptic input, which may play a key role in locomotor rhythm generation (MacLean, Cowley et al. 1998). In addition to 5HT, bath application of selective agonists for excitatory amino acid receptors, particularly NMDA and kainite receptors, demonstrated involvement in generating organized fictive locomotor rhythms (Cazalets, Sqalli-Houssaini et al. 1992). It must be mentioned that exogenous drug application to preparations to induce fictive locomotion does not mean the drugs play an endogenous role in generating locomotion (Cowley and Schmidt 1997).

Neurochemicals that induce locomotor-like patterns in the *in vitro* rat spinal cord have also been examined in eliciting fictive locomotion in the neonatal mouse spinal cord. Although the individual effects of these drugs on locomotor rhythmicity of the mouse spinal cord have been mixed, a combination of NMDA, 5HT, and DA has been documented to produce stable rhythmic alternating locomotor-like activity that can last for hours (Jiang, Carlin et al. 1999, Whelan, Bonnot et al. 2000). Selective application of 5HT and NMDA (± bicuculline) to spinal cervical or thoracic bath compartments evoked rhythmic lumbar VR activity in brainstem-spinal cord preparation (Cowley, Zaporozhets et al. 2008). This suggests that resident spinal neurons (propriospinal) may be more than passive channels for conveying descending signals to the periphery (Cowley, Zaporozhets et al. 2008) in rodents.

1.2.3 Use of *in vitro* rodent spinal cord to study mammalian locomotor circuitry

The network structure and arrangement of mammalian locomotor CPG components have been extensively studied in rodents (Barajon, Gossard et al. 1992, Kjaerulff and Kiehn 1996, Cina and Hochman 2000). Additionally, mouse models have allowed for genetic manipulation of interneuronal subpopulations to investigate their roles in locomotion (Goulding 2009). There is a better understanding of spinal interneurons, neural pathways, and interactions between multiple neuronal populations using newborn rats and mice (Jiang, Carlin et al. 1999, Whelan, Bonnot et al. 2000, Chopek, Nascimento et al. 2018, Chopek, Zhang et al. 2021). The *in vitro n*eonatal rat/mouse spinal cord has been established as an excellent model for studying the locomotor network's anatomical and functional organization in the mammalian spinal cord (Kiehn and Butt 2003).

1.3 Propriospinal Neurons

Propriospinal neurons (PSN) are a heterogeneous group of neurons that are widely distributed throughout the spinal cord. Propriospinal neurons, by definition, are those interneurons that originate, project, and terminate entirely within the spinal cord (Laliberte (Cowley, Zaporozhets et al. 2010, Laliberte, Goltash et al. 2019). The role of PSNs in the transmission of locomotor signals continues to be investigated. These neurons have been demonstrated to be sufficient to mediate lower limb locomotion after removing all long direct bulbospinal fibers (Cowley, Zaporozhets et al. 2008, Cowley, Zaporozhets et al. 2010). These resident spinal neurons appear to send and coordinate locomotor signals across varying distances (Cowley, Zaporozhets et al. 2008).

Although the role of descending commands in locomotion is well recognized, there is evidence of ascending propriospinal projections that appear to propagate motor signals (Viala and Vidal 1978, Magnuson and Trinder 1997, Ballion, Morin et al. 2001, Juvin, Simmers et al. 2005, Juvin, Le Gal et al. 2012, Zhang, Shevtsova et al. 2022). These studies have generally pointed towards propriospinal neurons mediating interlimb coupling and coordination between lumbar and cervical locomotor CPGs in quadrupeds. Despite propriospinal neurons being sufficient to mediate forelimb-hindlimb coordination, a synergistic interaction was recently observed between this signaling pathway and sensory afferents activated by lumbar dorsal root stimulation (Boulain, Khsime et al. 2021). This interaction between propriospinal pathways and sensory networks enhanced coordination between the cervical and lumbar locomotor generators in the isolated neonatal rat *in vitro* preparations (Boulain, Khsime et al. 2021). The nature, heterogeneity, and complex interactions of propriospinal neurons, including their ability to transmit signals across multiple spinal cord segments, make them a potential therapeutic target

for locomotor and possibly autonomic recovery after spinal cord injury (Cowley, Zaporozhets et al. 2010, Etlin, Blivis et al. 2010, Flynn, Graham et al. 2011, Cowley 2018).

1.4 Spinal Segments and Rhythmogenicity

The spinal locomotor system is complex. Several attempts have been made to clearly define the location and distribution of neural networks producing locomotor-like patterns in mammals. There still appears to be multiple interlinked neuronal pathways in the spinal cord that are involved in the generation of locomotor-like activity. However, specific lesioning and partitioning studies have given some insight into the regional organization of the spinal locomotor circuitry in vertebrates (Ho and O'Donovan 1993, Cazalets, Borde et al. 1995, Kjaerulff and Kiehn 1996). In chick embryos, the ability to generate hindlimb rhythmicity was more pronounced in the rostral lumbosacral spinal cord (Ho and O'Donovan 1993). Additionally, rhythm-generating networks in a transverse slice of embryonic chick spinal cord were demonstrated in the ventral region. This suggests that the primary elements of the CPG lie in the most ventral regions of the spinal cord (Ho and O'Donovan 1993, Kjaerulff and Kiehn 1996). Their lesion studies on neonatal rat spinal cord observed persistent rhythmic activity on lumbar VRs ipsilateral to the larger medial spinal fragment. However, isolated lateral spinal cord segments showed absent VR rhythmicity. These results indicate that rhythm-generating networks are likely concentrated medially than laterally in the lumbar spinal cord (Kjaerulff and Kiehn 1996).

Contrary to findings from Cazalet et al. 1995, several other studies have demonstrated that although the hindlimb CPG components are distributed over the entire lumbar spinal cord, caudal thoracic, and rostral lumbar segments are particularly rhythmogenic (Kjaerulff and Kiehn

1996, Cowley and Schmidt 1997, Kremer and Lev-Tov 1997, Magnuson and Trinder 1997). Studies that investigated the ability of the rostral and caudal lumbar spinal regions to generate hindlimb locomotor activity showed the former to have a higher propensity to generate regular rhythmic bursting (Deliagina, Orlovskii et al. 1983, Ho and O'Donovan 1993, Kjaerulff and Kiehn 1996). These results indicate that the spinal locomotor system is a distributed system with caudal thoracic (T13) and rostral lumbar (L1/L2) spinal segments being more critical to initiating and sustaining hindlimb locomotor activity than others.

Besides its significant role in initiating and controlling movement, the spinal cord can activate tissues and organs necessary to maintain body homeostasis under different locomotor demands. The latter functions are relegated to the domain of spinal autonomic systems.

1.5 Autonomic Nervous System

The autonomic nervous system (ANS) controls many involuntary bodily functions like sweating, blood pressure regulation, breathing, etcetera. This control system is classified into three major divisions: the sympathetic (SNS), parasympathetic (PNS), and enteric nervous systems. The enteric nervous system regulates the secretory and motor functions of the gastrointestinal tract. Many internal body organs receive a dual innervation from the sympathetic and parasympathetic neural networks (**Figure 1**), and both produce opposite effects on organs. However, both systems participate in maintaining body homeostasis in different environmental conditions. While the sympathetic system gets activated to prepare an organism for “fight or flight,” the parasympathetic primarily controls bodily functions for “rest and digest’. The output

of both sympathetic and parasympathetic systems generally comprises two sets of neurons, the preganglionic and postganglionic neurons.

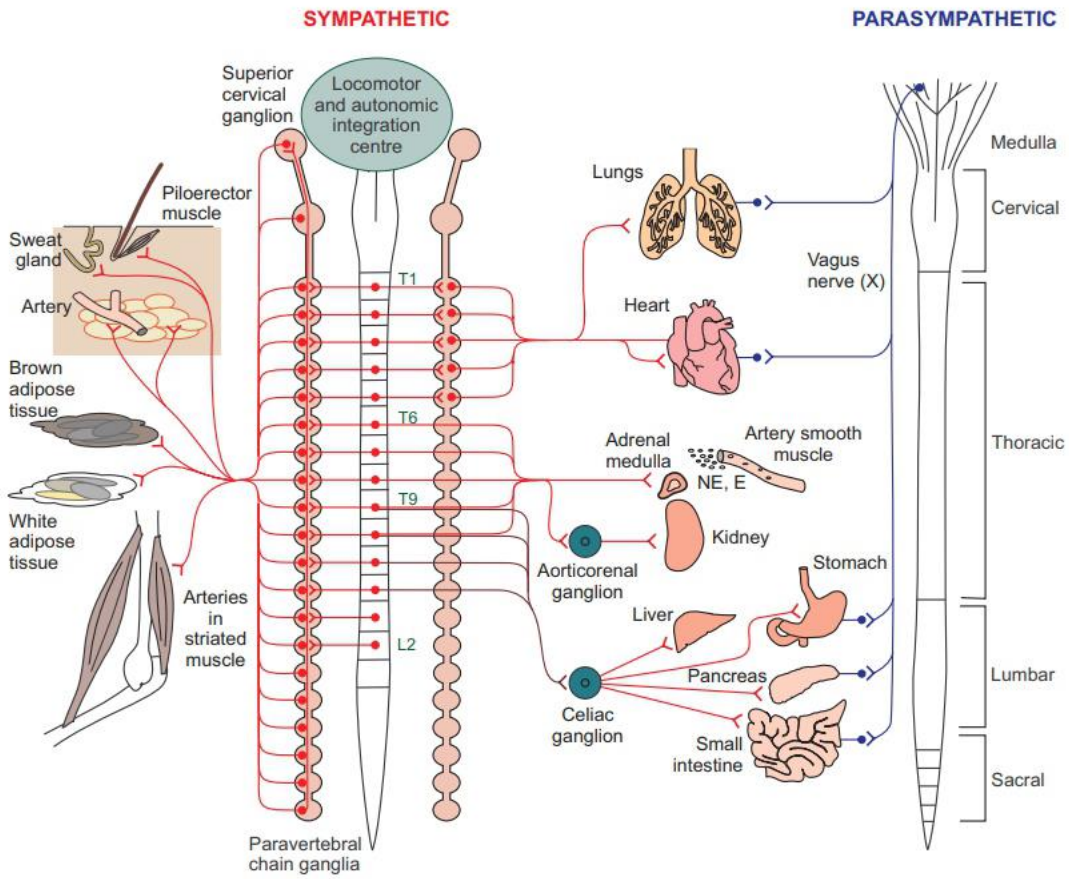

Cowley, 2018.

Figure 1: Organization of the sympathetic and parasympathetic nervous systems and their innervation of internal body organs. The two autonomic divisions have pre- and post-ganglionic neurons. SPNs arise from thoracic T1 to lumbar L2 segments, while the preganglionic PNS arise from the brainstem. Locomotion and exercise are severely impaired with SCI above the thoracic T1 segmental level.

1.5.1 Sympathetic Preganglionic Neurons

Sympathetic preganglionic neurons (SPNs) are the source of all central sympathetic neural input to the body (Deuchars, Spyer et al. 1995) and span from thoracic T1 segments to lumbar L2 segments (Cabot 1990). Their cell bodies lie in the intermediate region of the spinal cord and are organized into clusters called "nests." These nests are distributed among four subnuclei: the intermediolateral column (IML), intercalated nucleus, central autonomic area, and dorsolateral funiculus (Llewellyn-Smith and Verberne 2011). The IML contains most of the sympathetic preganglionic somata. These SPN cell bodies vary in shape and size but generally are 40-50% smaller than those of motoneurons and more prominent than those of dorsal horn neurons (Cabot 1990).

The somatotopic organization of SPNs has been demonstrated by injecting pseudorabies virus (PRV) into different body tissues and allowing retrograde labeling of SPNs projecting to the target tissues (**Table 2**). SPNs are topographically distributed along the length of the spinal cord. Although there is some overlap across spinal segments, generally speaking, neurons originating from upper thoracic segments (T1-T5/T6) provide sympathetic innervation to tissues and organs in the head, neck, and upper body like the lungs the heart (Loewy and Spyer 1990). In contrast, SPNs in the mid/caudal thoracic and upper lumbar spinal segments (T7-L2) supply the adrenals, kidney, splanchnic, and several other abdominopelvic structures (Sato 1987, Strack, Sawyer et al. 1988). Target tissues such as arteries, sweat glands, and adipose tissues are regulated by sympathetic neurons that arise from the thoracic and lumbar spinal cord (T1–L2), as shown in **Figure 1** (Cowley 2018). Sympathetic innervation of sweat glands generally follows body dermatomes (Nathan and Smith 1987). These targets were identified initially using pseudorabies virus and fluorescent dye labeling experiments (Strack, Sawyer et al. 1988,

Bamshad, Aoki et al. 1998, Smith, Jansen et al. 1998, Bamshad, Song et al. 1999, Adler, Hollis et al. 2012)**.** Axons of SPNs exit the spinal cord through ventral roots, and many form synapses onto postganglionic neurons that activate specific body tissues/ organs (Cabot 1990).

SPNs receive presynaptic input from supraspinal and spinal neurons in the intact spinal cord. Supraspinal input to SPNs has been identified using virus tracing techniques as the rostral ventrolateral medulla (RVLM), rostral ventromedial medulla (RVMM), A5 region, caudal raphe nuclei, and paraventricular nucleus of the hypothalamus. The spinal pre-ganglionic sympathetic neurons are found in rats' laminae V, VII, and X (Cabot 1990, Cabot, Alessi et al. 1994, Joshi, Levatte et al. 1995, Clarke, Dekaban et al. 1998, Tang, Neckel et al. 2004).

Injection site	Spinal segment														
	T1	T2	T3	T4	T5	T6	T7	T8	T9	T10	T11	T12	T13	L1	L2
Atrial myocardium	X	X	X	X	X	X									
Ventricular myocardium	X	X	X	X	X	X	X								
Brown adipose tissue			X	X	X	X									
Pineal gland	X	X	X												
Eye	X	X	X												
Pinna		X	X	X	X										
Adrenal gland		X	X	X	X	X	X	X	X	X	X	X	X		
Mammary Gland			X	X	X	X	X	X	X	X					
Kidney					X	X	X	X	X	X	X	X	X		
Spleen			X	X	X	X	X	X	X	X	X	X			
Ovary				X	X	X	X	X	X	X	X	X			
Uterus											X	X	X		
Prostate gland												X	X	X	X
Urethra														X	X
Seminal vesicles														X	X
Penis										X	X	X	X	X	X
Bladder														X	X
Colon													X	X	

Deuchars and Lall, 2015.

Table 2: Somatotopic organization of SPNs in the spinal cord. The table summarizes the spinal cord levels where PRV-infected sympathetic preganglionic neurons were found after PRV injections into different internal body tissues and organs.

1.5.2 Neurotransmitter Effects on SPNS:

Spinal and supraspinal presympathetic neurons contain a variety of neurotransmitters (NT), including monoamines, amino acids, and neuropeptides. While nerve terminals containing amino acid and neuropeptides originate from both the brainstem and spinal cord, those

containing monoamines originate exclusively from supraspinal sources (reviewed in Llewellyn-Smith and Verberne, 2011), like what has been observed for spinal motor systems (Holstege and Kuypers 1987, Newton, Burkhart et al. 1989, Maxwell, Riddell et al. 2000). These neurotransmitters and neuromodulators have been shown through immunohistochemical studies to occur in axon terminals that make synaptic contacts with SPNs. In line with this, electrophysiological studies have further demonstrated varying effects of the exogenous application of these neurochemicals to SPNs, as described below.

Amino acids like glutamate, gamma-aminobutyric acid (GABA), and glycine are thought to originate from both supraspinal and intraspinal sources. In spinal cord slice preparations, fast excitatory postsynaptic potentials (EPSP) were evoked in SPNs by stimulating different spinal regions (lateral funiculus, IML, dorsal horn, and dorsal rootlets) ipsilaterally or contralaterally. The observed SPN excitatory response to stimulation was wholly blocked by bath application of non-NMDA antagonists. Similarly, applying NMDA receptor antagonists to spinal cord slice preparations reduced the amplitude of SPN excitatory postsynaptic potentials evoked by stimulating the regions mentioned above. These results indicate the existence of presympathetic spinal neurons that use glutamate as a neurotransmitter acting via NMDA and non-NMDA receptors on SPN (Spanswick, Renaud et al. 1998). Krupp and Feltz (1995) also tested the function of glutamate receptors on the SPN membrane by exogenously applying agonists like NMDA to rat spinal cord slices. In their whole cell patch clamp recordings, NMDA induced inward currents in most tested SPNs at a holding potential of -30mV. Like Spanswick, Renaud et al. (1998), they also demonstrated that electrical stimulation of lateral funiculus or dorsal horn evoked EPSPs in recorded SPNs. The EPSPs were mediated by glutamate release onto SPNs (Krupp and Feltz 1995).

While studying the effect of NMDA on SPN, Mo and Dun noted that pressure application of exogenous NMDA in transverse SC slices evoked EPSPs and sometimes inhibitory postsynaptic potentials (IPSPs) in patched SPNs (Mo and Dun 1987, Dun and Mo 1989). Observed SPN membrane depolarization was thought to be a direct excitatory effect of NMDA on SPNs since the experiment was done with tetrodotoxin (TTX), a sodium channel blocker in the bath. In contrast, hyperpolarization was suggested to be due to an indirect excitation of spinal inhibitory neurons presynaptic to SPNs (Dun and Mo 1989). These NMDA-evoked IPSPs in SPN were abolished by strychnine or NMDA receptor antagonist, indicating that the IPSPs were due to glycine release from interneurons, which NMDA likely activates. This is consistent with EPSPs and IPSPs recorded in putative SPNs following superfusion of NMDA, kainate, and quisqualate in rat spinal cord slices (Spanswick and Logan 1990).

Unlike glutamate, glycine and GABA induce inhibitory responses in SPNs. Applying bicuculline (BIC), a GABA receptor antagonist, increased SPN firing frequency and excitability (Wang, Spary et al. 2008). In rat spinal slice preparation, electrical stimulation of interneurons in the central autonomic area (CAA) elicited IPSPs in SPNs in the IML region (Deuchars, Milligan et al. 2005). These evoked IPSPs in SPNs were abolished by adding bicuculline ($GABA_A$ receptor blocker) and/or strychnine, a glycine receptor blocker (Deuchars, Milligan et al. 2005). In the above experimental series, the reported SPN membrane potential response to CAA stimulation was likely a result of the direct effect of GABA and/or glycine on SPN receptors.

The effects of monoamines like norepinephrine (NE), epinephrine, and dopamine on SPN excitability have also been examined. Exogenous application of NE or epinephrine to adult cat spinal cord slices produced SPN membrane depolarisation in over one-half of recorded neurons and hyperpolarisation in less than a third (Inokuchi, Yoshimura et al. 1992). The remaining SPNs

produced biphasic (depolarisation-hyperpolarisation or vice versa) membrane responses with NE. In contrast, the superfusion of norepinephrine onto lateral horn cells in neonatal rat thoracolumbar spinal cord slices evoked only membrane depolarisation in identified SPNs (Ma and Dun 1985). This suggests that norepinephrine may be an excitatory monoamine in the rat spinal sympathetic network. On the contrary, bath application of dopamine agonists to transverse spinal slices of neonatal rats elicited both IPSPs and EPSPs, although IPSPs were the predominant SPN membrane potential response to dopamine (Gladwell and Coote 1999). Notably, the catecholamine-induced depolarisation or hyperpolarisation in SPN membrane potential may be attributed to changes (increase or decrease) in potassium conductance across the SPN membrane (Inokuchi, Yoshimura et al. 1992).

SPN excitability is also affected directly by serotonin. To examine the serotonin effect on SPNs, whole cell recording from SPNs in spinal cord slices revealed depolarising membrane potentials in 90% of recorded neurons (Pickering, Spanswick et al. 1994). The serotonin-evoked SPN excitation persisted in TTX. This indicates the presence of functional serotonin receptors on the SPN membrane and hence a direct effect of the drug on SPNs. It was also observed that the amplitude and duration of depolarization elicited in the SPN membrane were dose-dependent, with higher doses of 5HT inducing longer-lasting depolarisation of higher amplitude. Although serotonin generally overwhelmingly excited SPNs in the above study, a subpopulation of SPNs responded to serotonin by an initial inhibition followed by excitation (Pickering, Spanswick et al. 1994). This SPN subpopulation was located around the spinal cord's central canal. In other words, pressure ejection of serotonin over the IML region produced depolarising membrane response in SPNs, while biphasic responses were evoked in SPNs around the central canal. Interestingly, this biphasic inhibitory-excitatory SPN membrane response persisted in the

presence of TTX, suggesting inhibitory serotonin receptors on medial SPN dendrites. This is consistent with an earlier *in vivo* rat study where the iontophoretic application of serotonin agonists induced excitation in most SPNs and similar biphasic membrane responses in other recorded thoracic SPNs (Lewis and Coote 1990).

Unlike MNs, SPNs can generate spontaneous membrane potential oscillations. This ability was traditionally attributed to supraspinal influences on the spinal sympathetic network. However, SPN rhythmic behavior has been demonstrated in *in vitro* spinal cord experiments, suggesting a spinal origin. For instance, previously quiescent sympathetic preganglionic neurons developed membrane oscillations upon application of 5HT to rat spinal cord slices. Serotonin also increased the amplitude and frequency of rhythmic activity of spontaneously oscillating SPNs (Pickering, Spanswick et al. 1994, Pierce, Deuchars et al. 2010). These experiments' results suggest that serotonin induces or enhances SPN oscillatory behavior. The SPN oscillatory behavior is partly a function of spinal neurons coupled by gap junctions. This is because IML oscillations are attenuated by applying gap junction blockers, 18-glycyrrhetinic acid, mefloquine, or carbenoxolone (Pierce, Deuchars et al. 2010). Besides SPN responses to the application of neurochemicals, *in vitro* studies have equally demonstrated the response of these sympathetic neurons to electrical stimulation of regions within the brainstem and the spinal cord (reviewed in Deuchars and Lall, 2015).

1.6 Spinal Electrical Stimulation

In humans, there is currently no effective treatment to regain lost functions in SCI individuals. However, an emerging and promising treatment involves spinal electrical stimulation. Electrical stimulation (ES) has been successfully applied to the lumbosacral spinal cord after complete thoracic SCI to facilitate standing or stepping in animals (Courtine, Gerasimenko et al. 2009, van den Brand, Heutschi et al. 2012, Capogrosso, Wenger et al. 2013, Gad, Choe et al. 2013) and stepping in injured persons (Edgerton and Harkema 2011, Angeli, Edgerton et al. 2014, Kathe, Skinnider et al. 2022). In line with this, another study involving sensory, and motor complete SCI individuals showed that electrical stimulation of the lumbosacral spinal cord could promote effective standing without using assistive devices (Rejc, Angeli et al. 2015). Furthermore, Angeli and colleagues discovered that individuals with chronic paralysis following SCI could initiate voluntary leg movements with electrical spinal stimulation (Angeli, Edgerton et al. 2014).

Interestingly, in addition to improving motor function after SCI, electrical stimulation has also been used as an effective tool to concurrently improve autonomic functions previously lost following SCI. In their study, Harkema and colleagues 2018 reported that ES could safely raise blood pressure to normal levels in persons with SCI (Harkema, Wang et al. 2018). This is consistent with findings that reported normalized cardiac contractility and blood pressure with electrical spinal cord stimulation in individuals living with SCI (Phillips, Squair et al. 2018, Legg Ditterline, Aslan et al. 2021). ES has also been demonstrated to improve respiratory, sexual, bladder, and bowel functions as well as overall whole-body metabolism after spinal cord injury (Herman, He et al. 2002, Creasey and Craggs 2012, Hubscher, Herrity et al. 2018, Bloom, Wecht et al. 2020, Luo, Xu et al. 2020, Parittotokkaporn, Varghese et al. 2020).

The incidental finding that ES of the lumbar segments of the spinal cord simultaneously improves autonomic body functions and locomotor activity (Herman, He et al. 2002, Harkema, Legg Ditterline et al. 2018, Phillips, Squair et al. 2018, Nightingale, Walter et al. 2019, Legg Ditterline, Aslan et al. 2021, Flett, Garcia et al. 2022) poses the question of whether there is an interrelationship or connectivity between the locomotor neuronal network and spinal thoracic sympathetic control at the level of the spinal cord. This thesis is thus interested in examining how these two systems interact within the spinal cord.

1.7 Locomotor-related Neurons and the Sympathetic Circuitry

As humans engage in sustained rhythmic locomotor activities, such as cycling, skiing, running, and other forms of exercise, they require homeostatic and metabolic processes to support these endurance-based activities. The potential interactions between locomotor neural circuitry and neurons mediating sympathetic support to maintain sustained movement remain unknown. The question, therefore, is**:** What do we know about how or if these two spinal neural systems are integrated, and how does the sympathetic system get activated when we start to move?

Early researchers suggested physiologic mechanisms that lead to an increase in respiration during exercise. Some investigators viewed hyperpnea as a secondary effect of the exercise-induced increase in body temperature. Others proposed that the increase in ventilation occurred due to the parallel activation of locomotor and respiratory centers in the medulla (feedback vs. feedforward mechanism) (Eldridge, Millhorn et al. 1981). Eldridge and colleagues studied the relationship between locomotion and respiration in decorticate cats to validate the feedforward mechanism. They recorded increases in arterial pressure and respiration just before

the onset of spontaneous or induced locomotion in cats. This finding supported the idea of a feedforward parallel activation of locomotion and medullary cardiorespiratory centers during conditions of exertion, as posited by Krogh and Lindhard (Krogh and Lindhard 1913).

The current model of this feedforward mechanism is called “central command” and is described as the concurrent activation of neural signals to the motor and autonomic control during exercise (Koba, Kumada et al. 2022). The model has been further explored to demonstrate the neural pathways in the brainstem essential to drive somatic and sympathetic responses during sustained locomotor activity. Koba and colleagues and Stecina and colleagues used immunohistochemical and optogenetic stimulation techniques to identify the MLR-RVLM pathway as the vital connection through which the central command signals drive sustained locomotor activity and sympathetic responses (arterial pressure, heart rate, renal sympathoexcitation) in rats (Koba, Kumada et al. 2022, Armstrong, Nazzal et al. 2023) and see Figure 4B in (Cowley 2018).

In line with this, several other studies involving injection of retrograde tracer, PRV into various sympathetic tissues like the adrenal medulla, fat tissue, muscle, and cutaneous vasculature resulted in labeling of intermediate gray of the thoracic spinal cord as well as the RVLM (Strack, Sawyer et al. 1988, Bamshad, Aoki et al. 1998, Smith, Jansen et al. 1998, Bamshad, Song et al. 1999, Adler, Hollis et al. 2012). It is important to note that the results of these retrograde labeling studies provide the basis for direct SPN innervation of several sympathetic tissues. Hence, SPNs are a potential target for activation by neuronal populations originating from the brain or the spinal cord.

1.8 Project Rationale:

After SCI, there is a dysregulation of the autonomic nervous system with blunting of the sympathetic arm and dominance of the parasympathetic (Popa, Popa et al. 2010, Henke, Billington et al. 2022). This imbalance results in inadequate maintenance of body homeostasis and response to any disturbance in body equilibrium. Disrupting descending fibers from the supraspinal centers to the spinal sympathetic system ultimately leads to significant heart rate/rhythm irregularities, contractility issues, blood pressure fluctuations, and/or autonomic dysreflexia. It may also lead to copious respiratory secretions, thermoregulatory, bowel, bladder, and even sexual dysfunction in affected individuals (Garshick, Kelley et al. 2005, Furlan and Fehlings 2008, Wecht, Krassioukov et al. 2021, Henke, Billington et al. 2022). The extent of autonomic dysregulation in SCI varies with the level of injury. For instance, individuals with high lesions (T6 and above) suffer significant cardiovascular disturbances compared to those with low-level lesions (Furlan and Fehlings 2008). Cardiovascular dysfunction has recently been recognized as a leading cause of mortality in acute and chronic spinal cord injuries (Garshick, Kelley et al. 2005, Furlan and Fehlings 2008). Due to the importance of the ANS, recovery of autonomic functions and exercise tolerance rank very high on research priorities related to SCI (Anderson 2004, Phillips and Krassioukov 2015). The consequences of paralysis combined with autonomic dysfunction and reduced exercise capacity after SCI include obesity, early-onset type 2 diabetes, and cardiovascular disease in affected persons compared to the general population (Duckworth, Solomon et al. 1980, Lavela, Weaver et al. 2006, de Groot, Post et al. 2010).

We know that in neurologically intact individuals, the central command signal from supraspinal centers drives activation of sustained locomotor activity (e.g., exercise) and descending sympathetic outflow to metabolic tissues to maintain ongoing movement. However,

with SCI, there is disruption of these descending presympathetic fibers. Therefore, the spinal sympathetic circuitry would work to support locomotion independent of the brainstem command signal. Given the diverse functions of the spinal cord and extensive neuronal populations/ pathways therein, a new conceptual framework proposed the existence of possible intraspinal connections between the lumbar locomotor network and thoracic sympathetic neurons (Cowley 2018). The framework described the likelihood of the lumbar locomotor network communicating with thoracic SPNs through ascending propriospinal neurons. These potential ascending projections from lumbar locomotor neurons to thoracic SPNs may be key players in sustaining locomotion/ exercise after spinal cord injury (Cowley 2018, Flett, Garcia et al. 2022). As mentioned earlier, SPNs (i.e., source of all central sympathetic neural input to the body) span through thoracic and upper lumbar spinal segments and supply multiple tissues and organs in the body. This implies that some sympathetically regulated tissues (like the heart and adrenals) get activated during exercise to support ongoing movement. Other tissues like the gut and bladder become less active because they are not essential during physical exertion. It is also important to note that the concept of spinal locomotor-sympathetic integration may help explain why the use of epidural stimulation in human clinical trials simultaneously improves locomotor and autonomic functions after SCI.

As has been described, there are many parallels between neurotransmitters that activate locomotion and the origin of brainstem systems that project to either the thoracic spinal sympathetic neural networks and/or the cervical and lumbar motor networks. There is evidence that the sympathetic and motor systems are linked at the brain stem level (Strack, Sawyer et al. 1988, Bamshad, Aoki et al. 1998, Smith, Jansen et al. 1998, Bamshad, Song et al. 1999, Adler, Hollis et al. 2012). Strong evidence indicates that the spinal sympathetic and somatic motor

systems are functionally connected at the sensory afferent level and through intrasegmental and multisegmental somato-sympathetic spinal reflex responses (Sato 1997, Flett, Garcia et al. 2022). It is, however, not known whether direct intraspinal neural connections exist between the spinal sympathetic and motor systems.

We hypothesize that SPNs, through input from ascending propriospinal neurons, increase their activity during lumbar locomotor activity without descending input from the brain. We provide baseline data on SPN activity before and during lumbar locomotor activity by characterizing thoracic SPN activity patterns in the *in vitro* spinal cord preparation.

The results of this project will demonstrate the influence of lumbar locomotor activity on thoracic SPNs without supraspinal contribution. Further, it will provide novel insight into a functional intraspinal connection between lumbar locomotor-related neurons and SPNs. These findings may provide insight into the neural pathways that lead to improved motor and autonomic functions from spinal cord electrical stimulation.

1.9 Hypotheses and Aims of Study

1.9.1 Overarching Hypothesis:

Ascending propriospinal neurons from the lumbar locomotor network synapse on thoracic SPN and coordinate locomotor circuitry with sympathetic networks to ensure there is appropriate metabolic support during movement.

1.9.2 Specific Aims & Hypotheses:

1) Characterise the activity patterns of thoracic SPNs during tonic motor activity.
    a. **Hypothesis 1**: Thoracic SPNs demonstrate increased activity during tonic lumbar VR output.

2) Characterise the activity patterns of thoracic SPNs during rhythmic locomotor activity.
    a. **Hypothesis 2**: Thoracic SPNs demonstrate rhythmic activity during rhythmic lumbar VR output.

3) Determine if activity patterns of SPNs located in rostral thoracic spinal segments differ from SPNs in the caudal thoracic segments during lumbar locomotor activity.
    a. **Hypothesis 3**: A higher proportion of SPNs in the rostral thoracic segments (T1-T7) show increased activity compared to those in the caudal thoracic segments (T8-T13) during lumbar locomotor activity.

Chapter II: Materials and Methods

2.1 Ethics Declaration

The University of Manitoba Central Animal Care Committee approved the experimental protocols used in this study. Experiments were conducted per the guidelines set by the Canadian Council on Animal Care and the University of Manitoba.

2.2 Experimental Animal Model

Experiments were performed on newborn mice of C57BL/6 strain at 1–6 days old (P0 – 5). The C57BL/6 mouse model is popularly used in various areas of biomedical research, including neuroscience. Neonatal mice used in our series of experiments were bred at the Genetic Models Centre, University of Manitoba.

2.3 Spinal Cord Preparation

Twenty-six (26) spinal cord preparations were isolated from mice of both sexes and used for experiments. Mice were anesthetized with isoflurane (Fresenius Kabi Canada Ltd, ON, Canada), decapitated at the medullo-spinal cord junction, and then transferred to a sylgard-coated (Sylgard, Dow Corning, MI, USA) petri dish containing cold ($<4^0$C) oxygenated (95% O_2 and 5% CO_2) dissecting solution. The dissecting solution contains (in millimoles, mM) 215.0 Sucrose, 3.0 K-gluconate, 1.3 NaH_2PO_4, 26.0 $NaHCO_3$, 4.0 MgSO4-7H2O, 10.0 D-glucose, 1.0 Kynurenic acid and 1.0 $CaCl_2$. The decreased temperature is thought to reduce tissue metabolic rate and oxygen demand, resulting in better tissue survival (Bigelow 1958). Mice were pinned

down onto the dish with the ventral side facing up. The skin was removed, and mice were eviscerated with sharp scissors, exposing the vertebral column.

A ventral laminectomy was performed, ventral and dorsal roots were cut near the ganglia, and the spinal cord was removed from the vertebral column. The whole spinal cord (rostral cervical to caudal sacral) was then transferred to a 30ml sylgard-lined dish with oxygenated Ringers artificial cerebrospinal fluid (raCSF) warmed to room temperature (23-25^{0}C) containing (in mM) 111.0 NaCl, 3.0 KCl, 10.9 D-glucose, 25.0 $NaHCO_3$, 1.2 $MgSO4.7H_2O$, 2.5 $CaCl_2$ and 1.1 KH_2PO_4. The connective tissue surrounding the spinal cord was carefully removed using fine forceps to optimize oxygen diffusion through the preparation. The spinal cord was positioned with the ventral side facing upwards and secured using fine insect pins on the sylgard-bottomed chamber (**Figure 2a**). The preparation was continuously superfused with an oxygenated ringer's artificial cerebrospinal fluid.

2.4 Calcium Indicator Dye

Fluorescent calcium indicator dyes with calcium imaging technique have been widely and successfully used to monitor neuronal activity in both *in vitro* and *in vivo* experiments (McClellan, McPherson et al. 1994, Szokol and Perreault 2009, Tada, Takeuchi et al. 2014, Rancic, Haque et al. 2019, Zong, Obenhaus et al. 2022). These indicators are broadly grouped into chemically engineered fluorophores and genetically encoded fluorescent proteins (Paredes, Etzler et al. 2008). The chemically engineered fluorophores are available as salts, dextran conjugates, or acetoxymethyl (AM) esters. Each class has peculiar advantages and limitations (e.g., cell impermeability, dye sequestration or extrusion, phototoxicity, etc.). The preference for

one type of calcium indicator over the other depends mainly on the number and accessibility of investigated cells (Kettunen 2012). It is important to note that the use of calcium dye in monitoring neuronal activity is based on the established role of calcium in neuronal depolarization and action potential generation (McClellan, McPherson et al. 1994). In line with this, McClellan and colleagues showed that optical calcium signals recorded from the labeled brain and spinal cord neurons were abolished upon applying a calcium channel blocker. This indicates that the fluorescence signals emitted from cells of interest were due to an influx of calcium during electrically induced neuronal activity (McClellan, McPherson et al. 1994). We retrogradely labeled sympathetic preganglionic neurons for this study using Calcium Green Dextran Amine. This calcium indicator increases its fluorescence intensity following a rise in intracellular calcium level and calcium binding.

2.5 Neuronal Labeling with Retrograde Dyes

Crystals of calcium green conjugated dextran amine (CGDA; 3000 MW, Life Technologies Corp., OR, USA) were first reconstituted to a concentration of 20%. This was achieved by adding 25ul of raCSF to 5mg of CGDA crystals. Four to six microliters of reconstituted calcium dye were used per experimental animal. While spinal cord preparation in raCSF was continuously aerated, reconstituted crystals of calcium green conjugated dextran amine were applied to cut T4-T12 ventral roots on one or both sides of the spinal cord using glass suction electrodes with internal diameters 100-120 μM (**Figure 2b**). The ventral root selected for retrograde labeling was mainly based on the number of spared ventral roots after spinal cord dissection. Ventral roots were cut close to their exit from the spinal cord to allow minimal labeling time. Retrograde labeling of corresponding thoracic motoneurons and

sympathetic preganglionic neurons continued in the dark at room temperature for at least 3hrs (Szokol et al. 2008, 2009).

In one preparation, the differences in size and location of SPNs and MNs in the spinal cord were demonstrated by applying 25% tetramethylrhodamine (TMR) (dextran, tetramethylrhodamine, 10,000MW, Life Technologies Corp., OR USA) to cut ends of T8 and T9 VRs bilaterally. Like CGDA, neuronal labeling with TMR continued in the dark for 3 hours. After labeling, the spinal cord was fixed in 4% paraformaldehyde for 24 hours and cryoprotected in 30% sucrose in PBS at 4 ˚C. The thoracic spinal cord (T7-T10) was isolated and embedded in Tissue-Tek O.C.T Compound (Sakura), frozen, and cut transversely on a cryostat (CryoStar NX50 ThermoScientific; sections of 30 μm). Glass coverslips were placed over the sections before obtaining images on a Zeiss Axio Imager Z.2 upright microscope.

2.6 Spinal Cord Mounting for Optical and Electrophysiological Recording

A block of agar was prepared in advance (measuring 2mm high x 10mm wide x 15mm long) with one side angled with a scalpel at 30 degrees. The spinal cord (ventral side facing upwards) was then mounted on the agar. The corresponding labeled thoracic spinal segment was attached to the angled edge of the agar block with acrylic glue. The thoracic spinal cord at the level of the agar block was then sectioned using a vibratome (Leica Biosystems, Ontario, Canada) to expose the surface of the labeled thoracic segment. Following transection, the bottom of the agar block containing the spinal cord was then glued to a clean sylgard-lined recording chamber bubbling with oxygenated raCSF. The caudal end of the spinal cord was pinned to the chamber to further stabilize the preparation during recording. Afterward, the entire setup was

placed under the microscope. A gravity-dependent perfusion system (ValveLink 8.3, Automate Scientific Inc., CA, USA) was made to continuously deliver oxygenated raCSF from a reservoir (60ml syringe) to the 15ml recording chamber. Excess raCSF volume was removed from the recording chamber through tubing connected to a peristaltic pump (Minipuls 3 Peristaltic Pumps, Gilson, WI, USA) and back into the reservoir. This permitted the recirculation of calculated fluid volumes at any given time during the experiments.

2.7 Microscopy and Optical Imaging

The obliquely cut spinal cord surface mounted on the recording chamber was made to lay horizontally under the microscope equipped with epifluorescence (**Figure 2c**). This 'obliquely cut, face up' setup allowed for better visualization of larger and deeper portions of spinal cord grey matter (Szokol and Perreault 2009). Using the 5×|0.15 objective (Carl Zeiss Microscopy, NY, USA), a broader view of the cut surface was visualized, identifying the ventral and dorsal horns, central canal, and intermediate region. The spinal cord intermediate region was magnified using a 20×|1.0 wide-field water immersion objective (Carl Zeiss Microscopy, NY, USA). The SPNs were identified by their location in the intermediolateral nucleus, which sits at the lateral edge of the spinal cord grey matter, their cell body morphology (Deuchars and Lall 2015), and labeling with CGDA. Individual CGDA-labelled SPNs were selected as regions of interest (ROIs). The ROIs (i.e., SPN cell bodies) were then selected to record transient calcium fluctuations at high and low sampling frequencies using epifluorescence microscope (Axio Examiner.Z1, Carl Zeiss Microscopy, Gottingen, Germany). Typically, we captured calcium transients at 7.5Hz (5.3 s duration pulse), and neuronal (SPN, MN) activities were examined during baseline, tonic, and rhythmic VR activity. In some trials, optical imaging was done at a

40Hz sampling frequency (12.5s duration pulse). On average, each recording session lasted for 60-120 minutes.

Labeled SPNs emit a fluorescent signal when calcium enters the neuron correlating with an action potential, indicating neuronal activity. Changes in fluorescence intensity due to calcium transients within labeled SPNs were captured using a high-speed camera (Prime BSI Scientific CMOS camera, Photometrics, BC, Canada) capable of wide-field imaging of the entire IML. A TTL pulse was sent from the camera to the electrophysiological data capture program (Signal 7.1, Cambridge electronic devices, Cambridge, UK) to correlate calcium oscillations with ventral root recordings.

2.8 Induction of Fictive Locomotion and Electrophysiological Recording

Glass suction electrodes were made to record the lumbar ventral roots' electrical activity. In brief, thin wall, borosilicate capillary glass with microfilament (A-M Systems Inc., WA, USA) with outer and inner diameters of 1.2mm x 0.90mm, respectively, were first pulled using a vertical electrode puller (Narishige Scientific Instrument Laboratory, Tokyo, Japan). The sharp electrode tip was gently broken on a bench stone (Dan's Whetstone Company Inc., AR, USA) and fire-polished over a small compact alcohol burner (Boekel Industries Inc., PA, USA). The desired tip diameter was achieved with intermittent soft filing and fire polishing of the electrode tip. Ventral root (VR) activity was recorded by applying the tight-fitting glass suction electrodes (measuring between 120 to 130μM) to L2 and L5 VRs, which correlate to flexor and extensor phases of the step cycle, respectively (Zaporozhets, Cowley et al. 2006, Cowley, Zaporozhets et al. 2009). VR signals were assessed for baseline noise level (20-50 μV acceptable at 1000X Gain), amplified 10000X, band pass filtered at 30-3000 Hz (Custom SCRC amplifier) and

acquired at 2000 Hz with CED Power 1401 AD board and Signal software (Cambridge Electronic Devices, Cambridge UK).

Neurochemicals were prepared as concentrated stock solutions (1–20 mM) with saline and stored in vials in the freezer. For each experiment, stable fictive locomotion was induced by application of varying combinations of the fresh vials of 5-hydroxytryptamine (5-HT, Sigma-Aldrich Co, MO, USA; 10–50 μm), *N*-methyl-d-aspartic acid (NMDA, Sigma-Aldrich; 2–10 μm), dihydrokainic acid (DHK, Tocris Bioscience, Bristol, UK; 150-400 μm), bicuculline (BIC, Sigma-Aldrich; 10–40 μm) and dopamine (DA, Sigma-Aldrich, 50-100 μm). Individual neurochemical concentrations refer to final bath concentrations described previously (Cowley and Schmidt 1994, Cowley and Schmidt 1997, Cowley, Zaporozhets et al. 2008, Cowley, Zaporozhets et al. 2009, Cowley, Zaporozhets et al. 2010). Drugs were applied directly into a drug reservoir (60ml syringe) with calculated raCSF volume, constantly bubbling with 95% O_2/5% CO_2. Neurochemicals flowed under gravity from the reservoir into the recording chamber to excite the spinal cord. As described above, a closed loop was also maintained to keep drug concentrations stable. Drug-induced VR activity was considered locomotor-like if: *1)* L2 patterns on the left and right sides of the spinal cord were out of phase with each other, 2) L5 patterns on the left and right sides of the spinal cord are out of phase with each other and/or *3)* L2 and L5 VRs on the same side of the spinal cord are out of phase with each other (at least on one side) (Cowley and Schmidt 1994, Cowley, Zaporozhets et al. 2008). In some preparations, a single ventral root (L2 or L5) was rhythmically discharging with a persistent bursting pattern that did not necessarily alternate with the other suctioned ventral root. Washout was done as necessary during experiments. It entailed having a clean reservoir containing fresh oxygenated raCSF to

replace recording bath content with clean raCSF. Washout was done over 15-20 minutes to ensure that all neurochemicals were removed from the tissue preparation.

2.9 Data analysis:

Calcium response was analyzed using Slidebook software (Intelligent Imaging Innovations, USA), where the mean fluorescence intensity for each ROI was plotted in a graph over time. Due to prolonged exposure and recording period of neurons, there were alterations in the overall fluorescence of selected neurons over time. To account for these alterations, a region within the recording field of epifluorescence but away from CGDA-labelled neurons was selected in each experiment to serve as a point of reference (background) before analysis. Neuronal signals were then expressed as a change in average fluorescence relative to baseline fluorescence intensity in labeled neurons (Rancic, Haque et al. 2019). Baseline fluorescence intensity in each ROI was also normalized to 1, and intensity changes during VR locomotor activity were expressed as a percentage increase or decrease from the baseline**.** ROIs demonstrating an increase or decrease from baseline activity were identified based on a change in fluorescence intensity of 3% or more. ROIs that exhibited a change in fluorescence intensity less than 3% from their baseline were classified as having no change during tonic or rhythmic VR discharge. Ventral root signal files were converted to an appropriate binary format which was further analyzed using various software tools, the Axoscope software and custom software developed by the Spinal Cord Research Centre (SCRC) at the University of Manitoba. Calcium imaging and ventral root recording data were summarized, and statistics were done using the Microsoft Excel program.

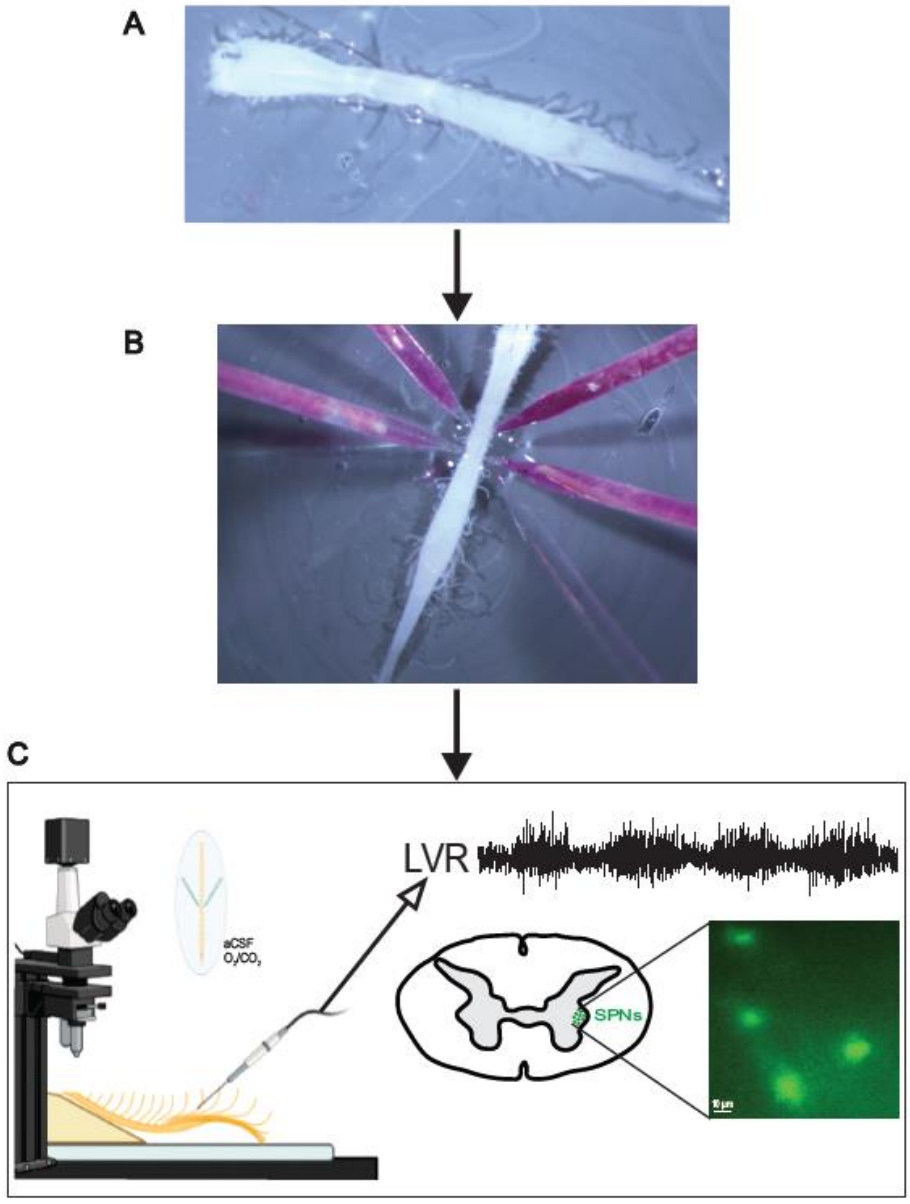

Figure 2: Schematic of experimental approach showing the whole spinal cord preparation (A), retrograde loading of calcium dye (B), spinal cord mounting, and optical recording of calcium responses during drug-induced VR activity (C).

Chapter III: Results

Fifty-two mice were used for experimentation, with data being collected and analyzed successfully from 26 of these mice. In 5 experiments, we examined the activity patterns of both SPNs and motoneurons in the same spinal preparation. In 20 experiments, we focused on only investigating SPN activity patterns. In a single preparation, we exclusively studied motoneuronal activity at baseline and during tonic and rhythmic ventral root activity. 26 spinal cord preparations were excluded from data analysis. 11 were excluded due to failure to induce ventral root activity with neurochemicals. 9 were excluded for software failure or technical problems during recording sessions. Furthermore, 6 were excluded during data analysis due to an unhealthy spinal cord cut surface and observed widespread soma swelling suggestive of neuronal death (Rousseau, Engelmann et al. 1999). Therefore, we analyzed SPN data from a total of 25 spinal preparations in a total of 34 trials. In one or two experimental trials, we examined neuronal activity for every animal during VR discharge. The number of trials per animal was determined by the extent of the viability of neurons on the exposed spinal surface and the overall health of the preparation.

3.1 Location of SPNs and Motoneurons:

To demonstrate the sizes and locations of sympathetic preganglionic neurons and motoneurons in the mouse spinal cord, we retrogradely labeled the neurons with tetramethylrhodamine (TMR) dye. Image obtained at 10x magnification showed dye uptake in the ventral root, labeled motoneurons in the ventral horn (VH) on both sides and tight clusters of labeled SPNs in the intermediolateral column on both sides (**Figure 3A**). The figure

demonstrates the larger somas of motoneurons (i.e., up to 50 μM diameter; **Figure 3B**) when compared to SPNs (i.e., up to 20 μM diameter; **Figure 3C**).

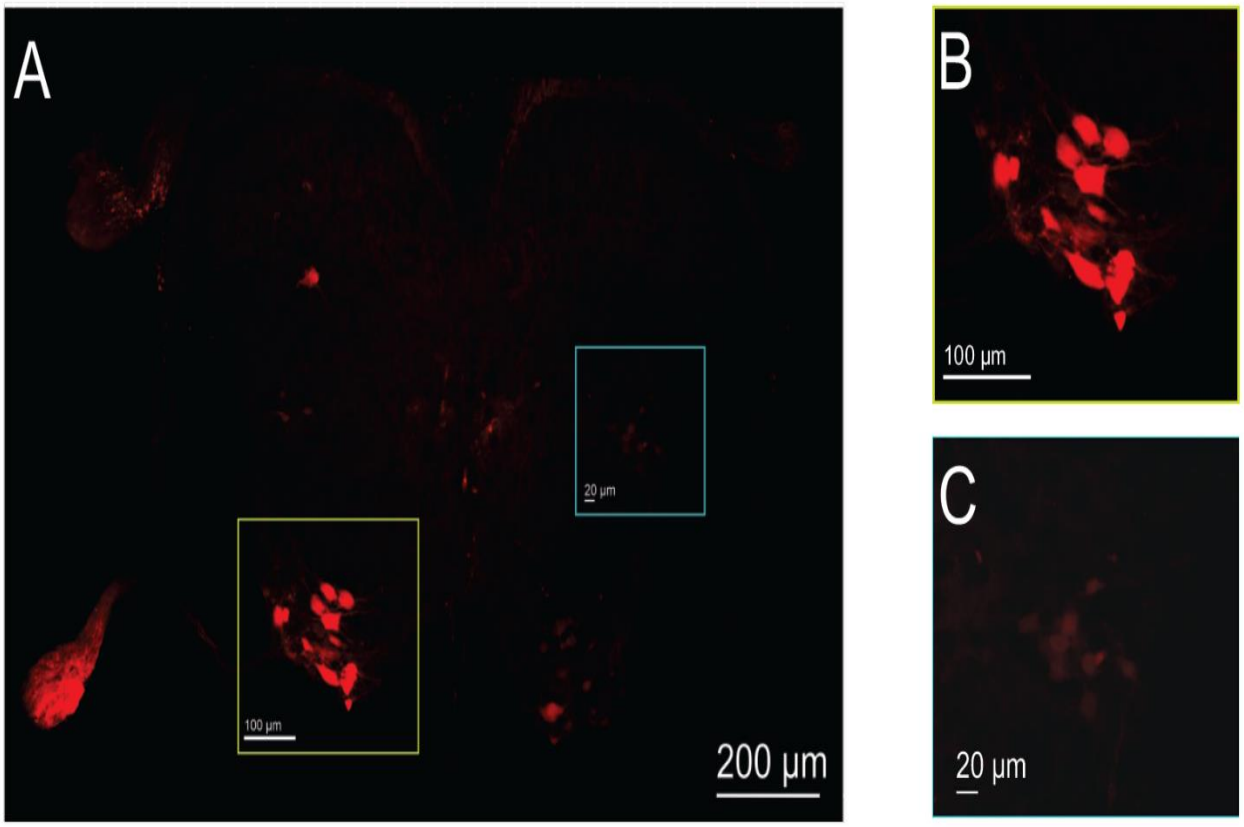

Figure 3: Location of SPNs and MNs within the mouse spinal cord. A) Low magnification image of 30μM section of the SC at T8 level showing location and morphology of retrogradely labeled neurons following TMR application to corresponding VR. The MN cell bodies are located in the SC's VH, while the neuronal clusters in the intermediate regions are the SPNs. Scale bar = 200μM. B) Magnification of the region within the light-green-colored box in panel A to show large somas of MNs. Scale bar =100μM. C) Magnification of the region within the teal-colored box to show the smaller SPN somas. Scale bar = 20μM, n = 1 (P4 mouse).

3.2 Neurochemical-Induced Ventral Root (VR) Activity in the Neonatal Mouse Spinal Cord

Locomotor-related lumbar neurons have been identified and characterized during neurochemical-induced fictive locomotor activity in an *in vitro* spinal cord preparation bent at an angle (Rancic, Haque et al. 2019). In our study, testing the ability to generate stable ventral root locomotor activity was necessary using the bent SC preparation. Initial experiments done with the spinal cord inclined at steeper angles (about 45 to 60 degrees) resulted in either no or frequently irregular lumbar VR locomotor activity. However, our rate of successfully generating stable rhythmic lumbar VR activity was increased upon altering the tilt angle of the spinal cord preparation to about 30 degrees. Thus, the isolated spinal cords were inclined at this angle on the agar block throughout the experimental series (see schematic in **Figure 2**).

Using twenty-six spinal cord preparations, we had forty trials of simultaneously recorded lumbar VR activity and SPN and/or MN calcium responses. Of the 40 lumbar VR recording trials, 12 exhibited stable rhythmic VR bursting upon applying a drug combination of 20-50μM 5HT, 2-10μM NMDA, and 50-100μM DA with or without bicuculline. Another six trials generated stable rhythmic VR bursting with 10-40μM 5HT, 50-400μM DHK, and 50-100μM DA combinations. We induced rhythmic VR activity in 36 out of our 40 trials. Only tonic VR discharge could be evoked with drugs in the remaining four trials. In 25/36 trials, 5HT evoked an initial tonic discharge followed by the appearance of rhythmic activity within 2-8 minutes. While a tonic increase in some trials preceded VR rhythmicity, rhythmic bursting appeared without an intermediate tonic discharge in 11/36 trials. The ventral roots targeted for recording were flexor-dominated L2 and extensor-dominated L5 VRs on both sides of the spinal cord. However, in some preparations, other ventral roots, such as L3 and L6, were suctioned for recording, depending on the availability and viability of roots. Ventral root recordings were taken from RL5

and LL5/6 (n=20), RL3 and LL5/6 (n=2), RL2 and LL2 (n=1), RL2 and LL6 (n=1), RL2 and LL3 (n=1) and RL3 and LL3 (n=1).

We observed spontaneous ventral root discharge (**Figure 4A**) in 15 of the 26 spinal preparations after suctioning lumbar VRs for recording. Different VR rhythmic patterns were induced using several drug combinations. The first drug-induced motor pattern is shown in (**Figure 4B**) and consisted of rhythmic activity alternating between left and right sides of the spinal cord (RL5 and LL5 in 7 trials; RL2 and LL2 in 1 trial). The second type of pattern consisted of synchronous bursts of activity (**Figure 4C, 4D**) in the ventral root on both sides of the spinal cord (RL3 and LL6 in 1 trial; RL5 and LL5 in 2 trials). Synchronous activity from RL3 and LL6 can be explained on the basis that L3 is flexor-dominated and L6 extensor-dominated. In the case of synchronous activity from L5 ventral roots bilaterally, bicuculline had been added to the neurochemical cocktail in the bath, which is known to induce synchronous rhythmic discharge (Cowley and Schmidt 1997). Other types of rhythmic VR discharge observed can be grouped as "irregular patterns" as there was a failure to elicit an organized pattern of rhythmic discharge during trials (n=14) (**Figure 4E, 4F**). In some trials, the generation of rhythmic VR activity was restricted to one side of the cord (10 trials; **Figure 4G**). This was most likely linked to the health of the other suctioned ventral root at the time of recording. As this is the first characterization of SPN patterns during rhythmic VR activity, we recorded SPN calcium responses during all observed VR motor patterns. The average time elapsed from recorded baseline VR activity to tonic or stable rhythmic discharge appearance ranged from 11 to 20 minutes. Of the different drug combinations used in our experiments, perfusing the mouse spinal cord with 20μM 5HT, 5μM NMDA, and 50μM DA cocktail was most consistent at eliciting stable locomotor-like activity in lumbar ventral roots.

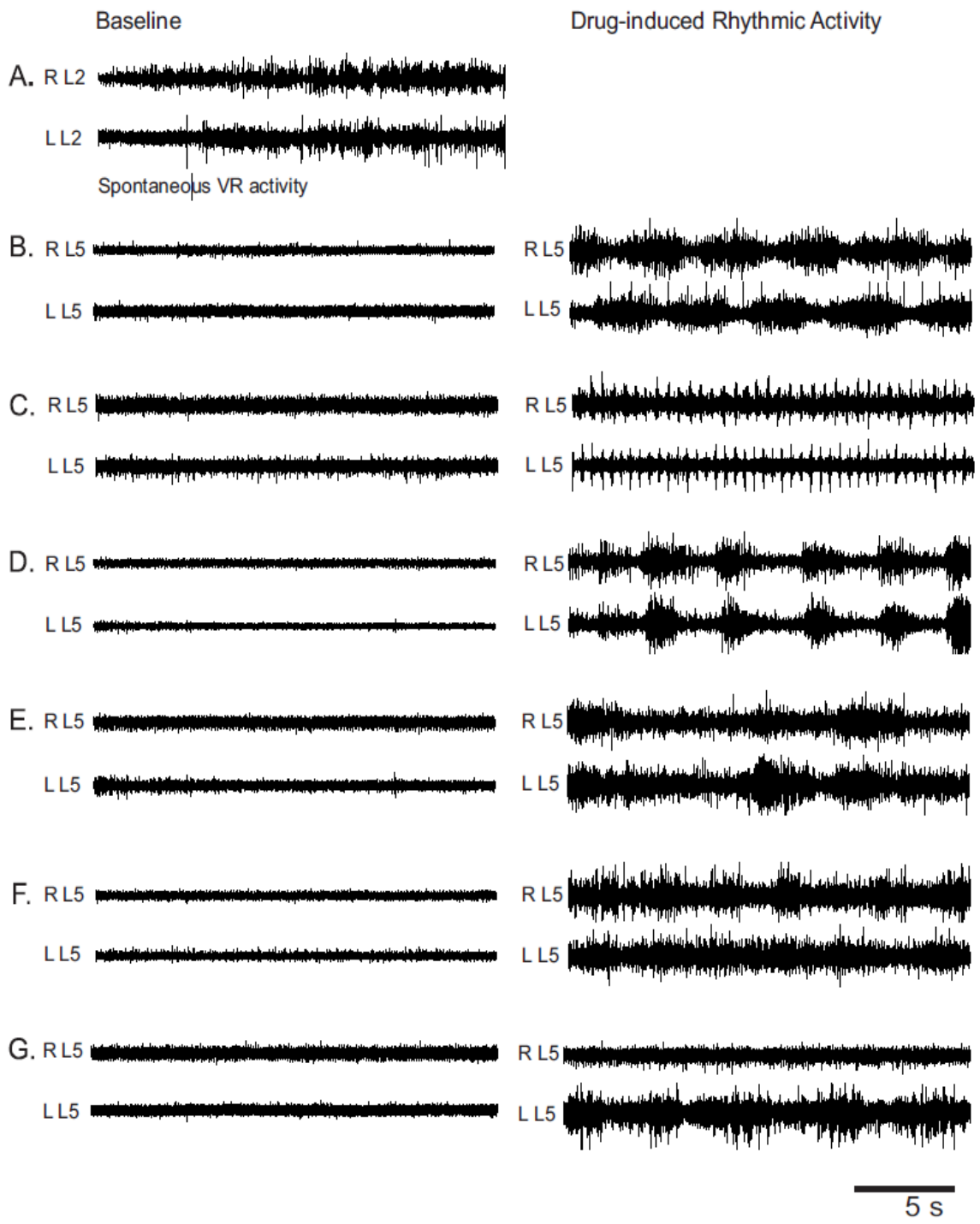

Figure 4: Examples of spontaneous and drug-induced rhythmic VR activity. A) Spontaneous discharge on the right L2 and left L2 VRs (P2 mouse). B) Locomotor-like activity consisting of a rhythmic alternation of contralateral L5 VRs (P3 mouse), induced with 5HT (20μM), DHK (200μM), NMDA (5μM), and DA (50μM). C) High-frequency synchronous rhythm in bilateral L5 VRs (P4 mouse) induced with 5HT (20μM), DHK (150μM), NMDA

(10μM), DA (100μM), and BIC (20μM). D) Synchronous rhythmic activity recorded at a lower frequency in bilateral L5 VRs (P5 mouse) by 5HT (20μM), DHK (200μM), DA (50μM), and BIC (20μM). E & F) Irregular rhythmic motor patterns in bilateral L5 VRs induced with 5HT (10-20μM), DHK (150-200μM), and DA (50-100μM) in P5 and P4 mice, respectively. G) Rhythmic activity in the presence of 5HT (40μM), NMDA (10μM), DA (100μM), and BIC (40μM) restricted to left L5 VR (P2 mouse).

3.3 Motoneurons Demonstrate Rhythmic Oscillations During Lumbar Locomotor Activity

Next, we tested the ability to use fluorescence calcium imaging to visualize cells and characterize their neuronal activity before and during fictive locomotion. As motoneurons are known to be rhythmically activated during locomotion, we tested our methods by retrogradely labeling motoneurons with CGDA at T10/T11 spinal segments. After the 3-hour incubation, the spinal cord was cut at the corresponding spinal segment, and the exposed CGDA-labeled motoneurons in the ventral horn were visualized. Although both MNs and SPNs were labeled, this experiment was restricted to recording neuronal activity (i.e., calcium responses) in motoneurons before and during lumbar VR activity. In this particular experiment, 22 labeled VH neurons were visually identified and selected as regions of interest (**Figure 5A**). L5 ventral roots were suctioned bilaterally for monitoring fictive locomotion. In this experiment, calcium responses were captured at both low (7.5 Hz) and high (40 Hz) sampling frequencies. The ROIs were recorded during baseline lumbar VR activity (i.e., without neurochemicals in the bath; **Figure 5D$_1$**). Tonic discharge was then evoked in the right L5 VR (**Figure 5D$_2$**) in response to 20μM 5HT, 5μM NMDA, and 50μM DA application. MN calcium responses were captured during tonic ventral root activity. Doubling the dose of the drug cocktail transitioned VR activity to a stable regular rhythmic bursting pattern (**Figure 5D$_3$**). The activity of all 22 MNs was then

recorded during VR activity (**Figure 5B**). Afterward, a washout was done to remove all neurochemicals from the bath and VR activity returned to baseline.

During baseline ventral root activity, no spontaneous calcium oscillations were observed in the motoneurons (**Figure 5E$_1$**). The MNs did not demonstrate calcium oscillations during the tonic activity until the VR output transitioned to a rhythmic pattern. As seen in **Figure 5E$_2$**, rhythmic oscillations began to appear in MNs towards the end of the recording frame, which coincided with or slightly preceded the onset of VR rhythmic activity. The calcium oscillations persisted in MNs throughout ventral root rhythmicity; however, the oscillatory patterns of the individual ROIs were different. Some ROIs showed more oscillations at the beginning of the frame and less towards the end and vice versa (**Figure 5E$_3$**). The difference in oscillatory behaviors observed in the individual MNs may be related to their excitability variations and recruitment pattern during motor output (Menelaou and McLean 2012). The oscillations in the MNs gradually disappeared upon washout. With the return of VR activity to baseline, there were no observed calcium oscillations in the motoneurons.

Regarding mean calcium intensity changes during tonic VR activity, most MNs showed an increase relative to their baseline calcium intensity values (**Figure 5C, 5F**). However, with the onset of rhythmic VR activity, most MNs demonstrated decreased calcium intensities compared to intensities during tonic activity despite displaying rhythmic calcium oscillations (**Figure 5C, 5F**). These results show that motoneurons are activated and are involved in fictive locomotor activity. The ability to record calcium responses in motoneurons and ventral root activity simultaneously established the feasibility of our experimental design. It is also interesting to note that many of these intensity changes represented only very slight increases, or decreases in intensity, typically of less than 5%.

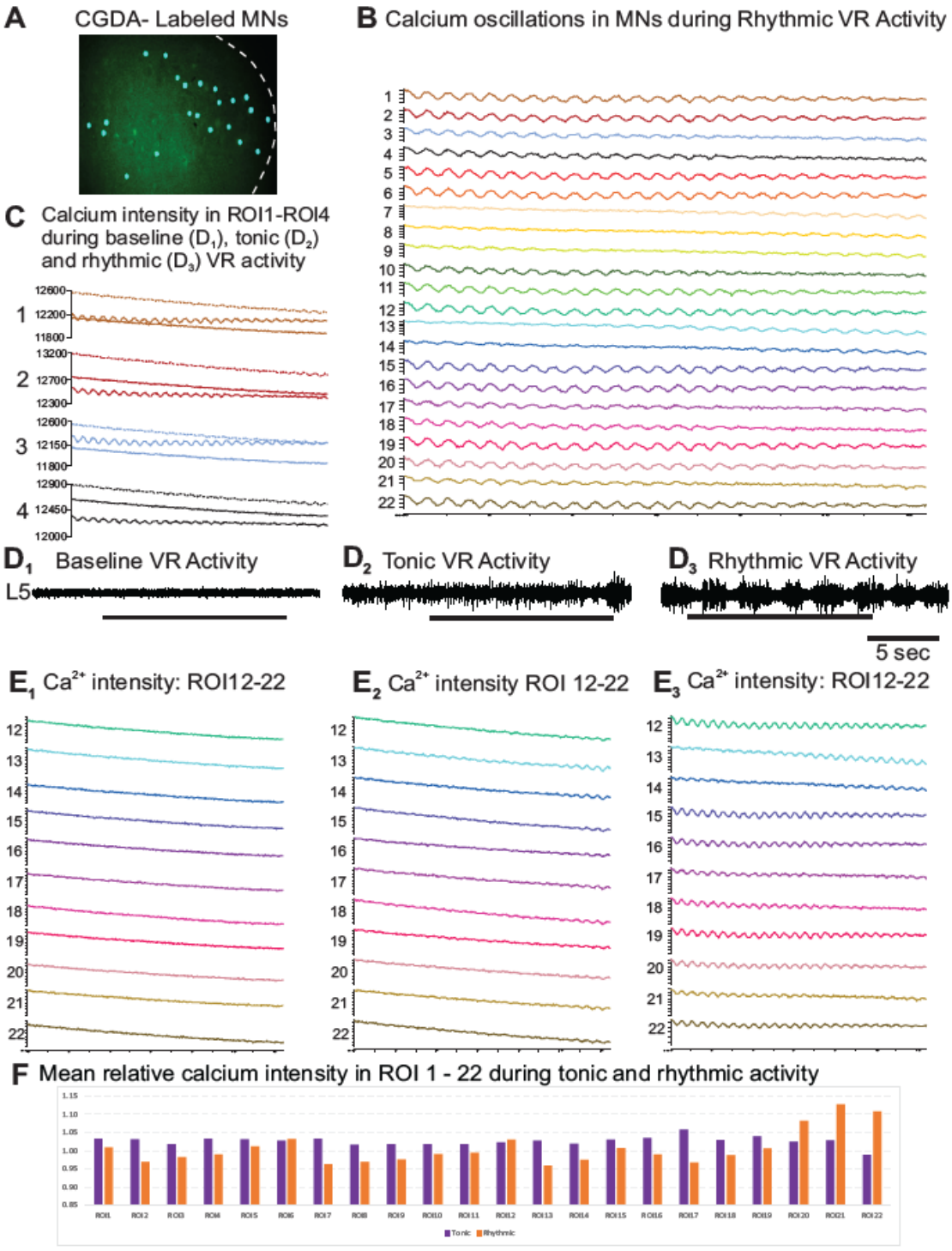

Figure 5: Motoneurons demonstrate rhythmic oscillations during lumbar locomotor activity. A) Masked regions represent selected ROIs (i.e., MNs) in the VH preloaded with the fluorescent calcium dye (P1 mouse; T10/T11 recording level; sampling frequency = 40Hz). B) Rhythmic calcium oscillations elicited in 22 MNs during drug-induced rhythmic VR activity. C) MNs showed an increase (dotted line graphs) and then a decrease (rhythmic line graphs) relative

to their baseline fluorescence intensity (solid non-rhythmic line graphs) during tonic and rhythmic VR activity, respectively. D) L5 VR recording at baseline (D_1) during drug-induced tonic (D_2) and rhythmic (D_3) activity. E) Calcium response of 10 selected MNs at baseline (E_1), during tonic (E_2), and rhythmic (E_3) ventral root activity. F) A bar chart illustrating mean calcium intensity changes in all 22 ROIs during tonic (purple) and rhythmic (orange) VR relative to baseline intensity. The baseline fluorescence intensity in each ROI was normalized to 1.

3.4 SPN Activity Patterns During Tonic Ventral Root Activity

Tonic ventral root discharge is described as a generalized increase in the excitation of spinal locomotor-related interneurons and motoneurons (Jean-Xavier and Perreault 2018). In 23 experiments, bath application of neurochemicals elicited tonic discharge in ventral roots. Because tonic VR discharge suggests increased excitation of the spinal locomotor circuitry (Jean-Xavier and Perreault 2018), we recorded SPN activity patterns during tonic VR discharge. There is currently a paucity of data describing the activity of SPNs during drug-evoked tonic discharge in ventral roots. In all 40 trials (n=26), an initial tonic discharge was elicited in 25 trials, followed by the appearance of rhythmic activity. In another four trials, tonic VR discharge persisted for the recording duration and did not switch to rhythmic responses. In most of these sessions, SPN calcium responses were captured at baseline (**Figure 6A**) and during tonic VR activity (**Figure 6B**) with a sampling frequency of 7.5 Hz. Some SPNs showed an increase in their fluorescence during tonic ventral root discharge. Others demonstrated a decreased intensity or remained the same as the baseline fluorescence (**Figure 6C, 6D**).

For all experiments, a change in SPN fluorescence intensity of 3% or more relative to the baseline fluorescence was considered a change in intensity level in identified SPNs. SPNs that displayed less than a 3% change from their baseline fluorescence intensity were considered to have shown no change in intensity with tonic or rhythmic VR discharge. With the appearance of

tonic VR activity in our first set of experimental trials, 182 SPNs were examined. Using the 3% cut-off value, 51/182, or 28% increased, 35/182 or 19% decreased, and 96/182 or 53% remained the same. In our second set of trials, 49 SPNs were recorded. Of this number, 19/49 or 39% increased, 4/49 or 8% decreased, and 26/49 or 53% remained the same.

Taken together, a total of 231 SPNs were examined during tonic VR activity. Approximately 30% of these demonstrated a mean percentage increase in fluorescence (of 5.5 % ± 2.8% SD), and 17% showed a mean percentage decrease (of 4.0% ± 1.5% SD) from the baseline fluorescence. Our results indicate that the percent increase and decrease in SPN activity during tonic VR activity were in the range of 3-15% and 3-9%, respectively. As reported below, the proportion of SPNs with increased or decreased activity varied across the different thoracic spinal segments (**Table 3**).

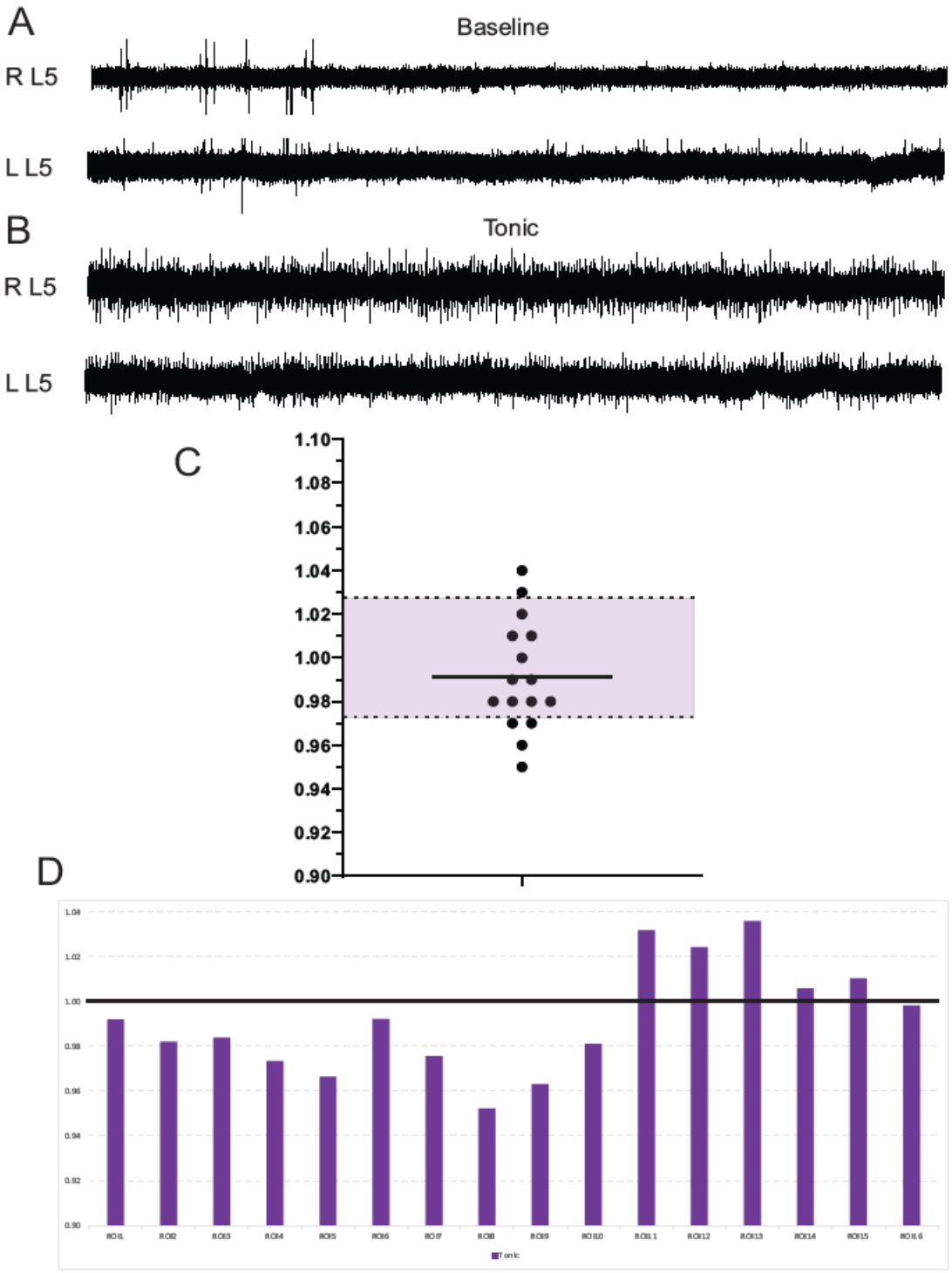

Figure 6: SPN activity patterns during tonic VR activity. ENG recording in the right and left L5 VRs at baseline (A) and during tonic activity (B) induced with 5HT (20μM), NMDA (5μM), and DA (50μM). C) The chart shows a grouped mean with individual SPN relative calcium intensity change during tonic VR. The shaded purple area represents a 3% arbitrary 'range' of no change. Data points above and below the purple area showed increased and decreased calcium

intensities, respectively. D) The bar chart illustrates mean calcium intensity changes in the 16 recorded SPNs during tonic VR relative to baseline intensity (normalized to 1)—P2 mouse; T9 recording level.

Rostrocaudal Spinal Level of Calcium Imaging	Number of Preparations	Number of SPNs with increased intensity of Calcium Response (Tonic VR)	Number of SPNs with decreased intensity of Calcium Response (Tonic VR)	Percent (%) with Increase	Percent (%) with Decrease
T4/T5	1	9/14	2/14	64	14
T6/T7	1	16/16	0/16	100	0
T7	1	4/4	0/4	100	0
T7/T8	2	1/13	6/13	8	46
T8/T9	5	14/53	13/53	26	25
T9	1	2/16	4/16	13	25
T9/T10	9	10/68	10/68	15	15
T10/T11	4	10/43	3/43	23	7
T12/T13	1	0/4	0/4	0	0

Table 3: **Summary of SPN calcium intensity changes during tonic ventral root discharge at different rostrocaudal thoracic levels.**

3.5 SPN Activity Patterns During Rhythmic Ventral Root Activity

Using the whole-cell patch clamp recording technique, the spontaneous and drug-induced rhythmogenic capability of SPNs has been demonstrated in rat transverse spinal cord slices (Logan, Pickering et al. 1996, Pierce, Deuchars et al. 2010). However, there is a lack of data investigating population responses of SPNs in the whole spinal cord preparation at baseline and during drug-induced fictive locomotion. To this end, we first examined SPN and MN calcium responses in the same spinal preparation (n=5) during baseline and rhythmic VR activity. In the above five preparations, 34/55 (62%) recorded SPNs showed spontaneous calcium oscillations at baseline VR activity (**Figure 7A, 7D**). These oscillations became greater during drug-induced fictive locomotion (**Figure 7C, 7D**). In contrast, the motoneurons exhibited small or no rhythmic oscillations at baseline and tonic VR activity but became rhythmic during fictive locomotion (**Figure 7F-I**). Additionally, changes in Ca^{2+} oscillations during the rhythmic locomotor activity appeared to be greater in SPNs than in MNs in this preparation (**Figure 7D vs. 7I**). In other words, SPNs demonstrated higher amplitude calcium oscillations than MNs during rhythmic VR activity. We also observed greater variability in the activity patterns of SPNs (**Figure 7D$_{1-4}$**) compared to MNs in our five preparations. As illustrated in **Figure 7I$_{1-4}$**, the absolute fluorescence intensities of MNs at baseline are not vastly different from their fluorescence intensities during tonic and rhythmic VR activity. This is why the MN absolute intensities during those VR conditions seem close to each other on their calcium plots. In contrast, changes in absolute intensity in SPNs are more variable during tonic and rhythmic VR activity, hence the much wider scale of calcium responses.

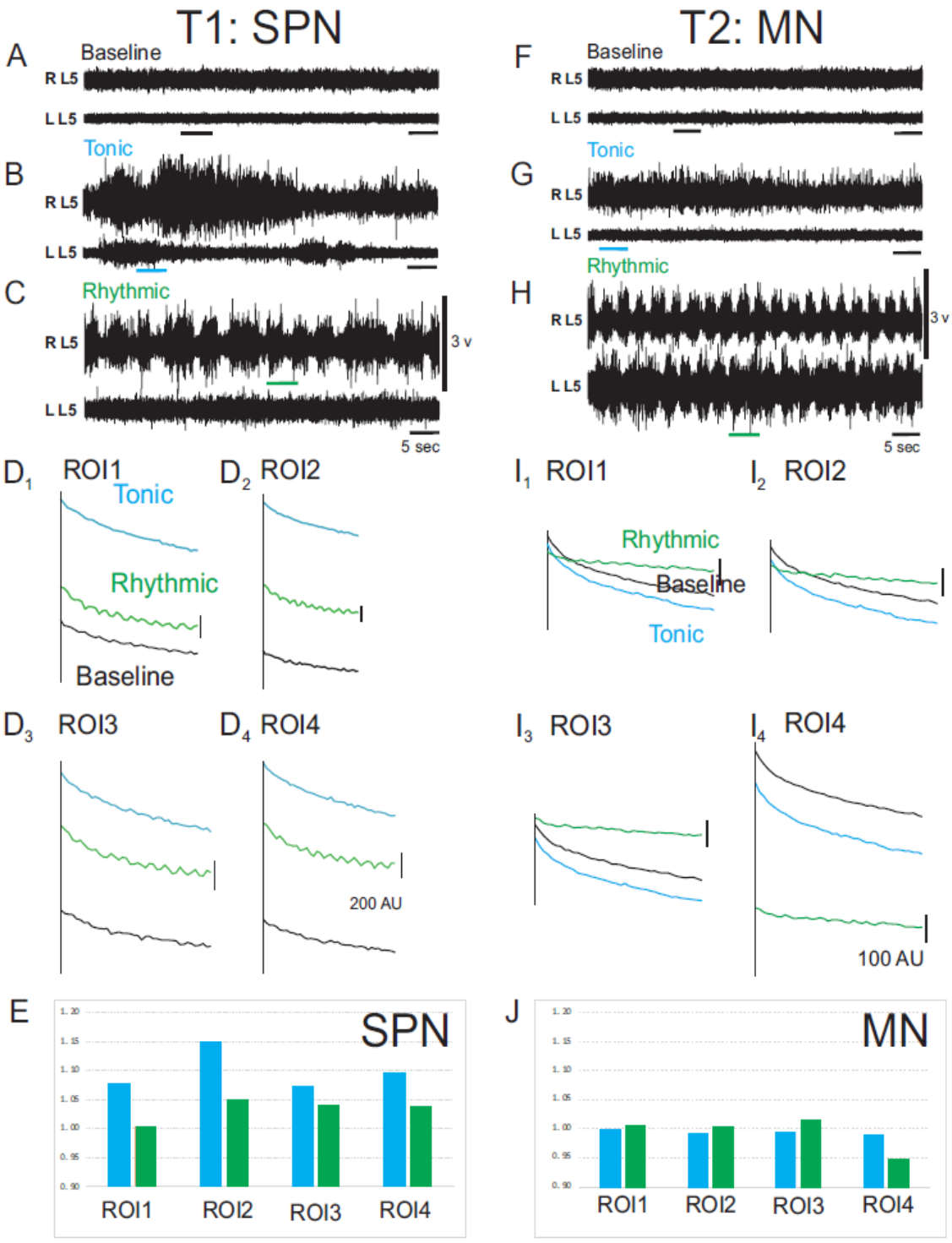

Figure 7: Example of SPN and MN behaviors at baseline, tonic, and rhythmic VR activity in the same preparation. SPN calcium responses were recorded in the first trial (T1), while MN calcium responses were recorded in the second trial (T2). **SPN:** During baseline VR activity (A), all 4 recorded SPNs (D_1-D_4) demonstrated spontaneous calcium oscillations, which became greater during rhythmic VR activity. The calcium graphs in both trials represent the absolute

change in calcium intensity levels in each ROI at baseline (black line graphs), during tonic (blue line graphs), and rhythmic (green line graphs) VR. As depicted in D_1-D_4, the calcium graph for each SPN demonstrated an increase in intensity relative to their baseline during tonic VR (B), with a comparatively lesser increase observed during rhythmic VR activity (C). **MN:** The 4 recorded MNs (I_1-I_4) showed no rhythmicity at baseline VR (F) and during tonic VR (G) but became rhythmic during rhythmic VR activity (H). Changes in Ca^{2+} intensity during tonic VR and changes in Ca^{2+} oscillations during rhythmic locomotor activity are greater in SPNs (scale = 200AU) than MNs (scale = 100AU) in this preparation. P2 mouse; T7 recording level; sampling frequency = 7.5Hz.

In other preparations, we recorded only SPN calcium responses at baseline VR activity (**Figure 8A**) and during rhythmic VR activity (**Figure 8B**). Regarding calcium intensity change in recorded SPNs during fictive locomotion, some SPNs demonstrated an increase from their baseline fluorescence intensities. Others showed either a decrease or no change in intensity (**Figure 8C, 8D**).

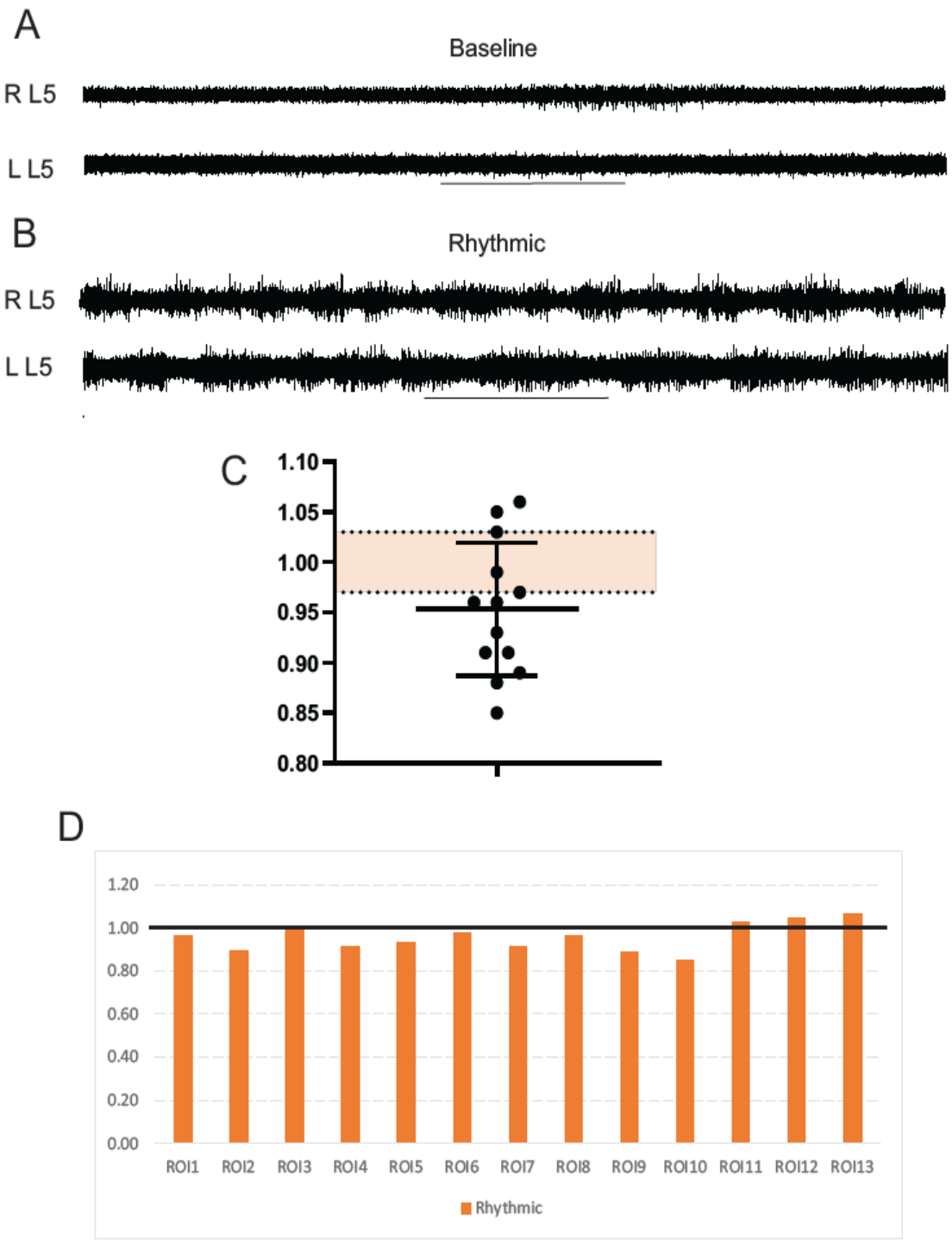

Figure 8: SPN activity patterns during rhythmic VR activity. ENG recording in the right and left L5 VRs at baseline (A) and during rhythmic activity (B) induced with 5HT (40µM), DHK (400µM), and DA (50µM). C) The chart shows a grouped mean with individual SPN relative calcium intensity change during rhythmic VR. The shaded orange area represents a 3% arbitrary 'range' of no change. SPNs above and below the orange region showed increased and decreased

calcium intensity, respectively. D) The bar chart illustrates mean calcium intensity changes in the 13 recorded SPNs from the T9/T10 segment during rhythmic VR relative to baseline intensity (normalized to 1); P2 mouse.

In some experiments, all SPNs recorded during tonic and rhythmic VR showed increased calcium intensity relative to their baseline values (**Figure 9**). Altogether, we recorded, in our first set of trials, 168 SPNs at baseline and during rhythmic VR activity. 40/168 SPNs increased their mean fluorescence intensity (24%) during drug-induced fictive locomotion, and 40/168 SPNs showed a mean decrease (24%) from their baseline fluorescence. The remaining 88 SPNs showed no change from their baseline fluorescence (52%). A total of 109 SPNs were recorded in our second set of trials with the same 25 spinal preparations. Of the 109 labeled SPNs, we observed an increase from baseline fluorescence intensity in 27 SPNs (25%) during VR rhythmic locomotor activity, a decrease in intensity in 7 SPNs (6%), and no change in 75 SPNs (69%)**.**

Taken together, out of 277 SPNs examined during fictive locomotion, approximately 24% demonstrated a mean percentage increase in fluorescence (of 7.4% ± 6.4% SD), and 17% showed decreased fluorescence intensity (of 5.5% ± 3.1% SD) compared to their baseline data. Our data showed that the percent increase and decrease in SPN activity during rhythmic VR were in the range of 3-33% and 3-15%, respectively. Like tonic activity, the proportion of SPNs with increased or decreased fluorescence varied across the different thoracic spinal segments, as described below (**Table 4**).

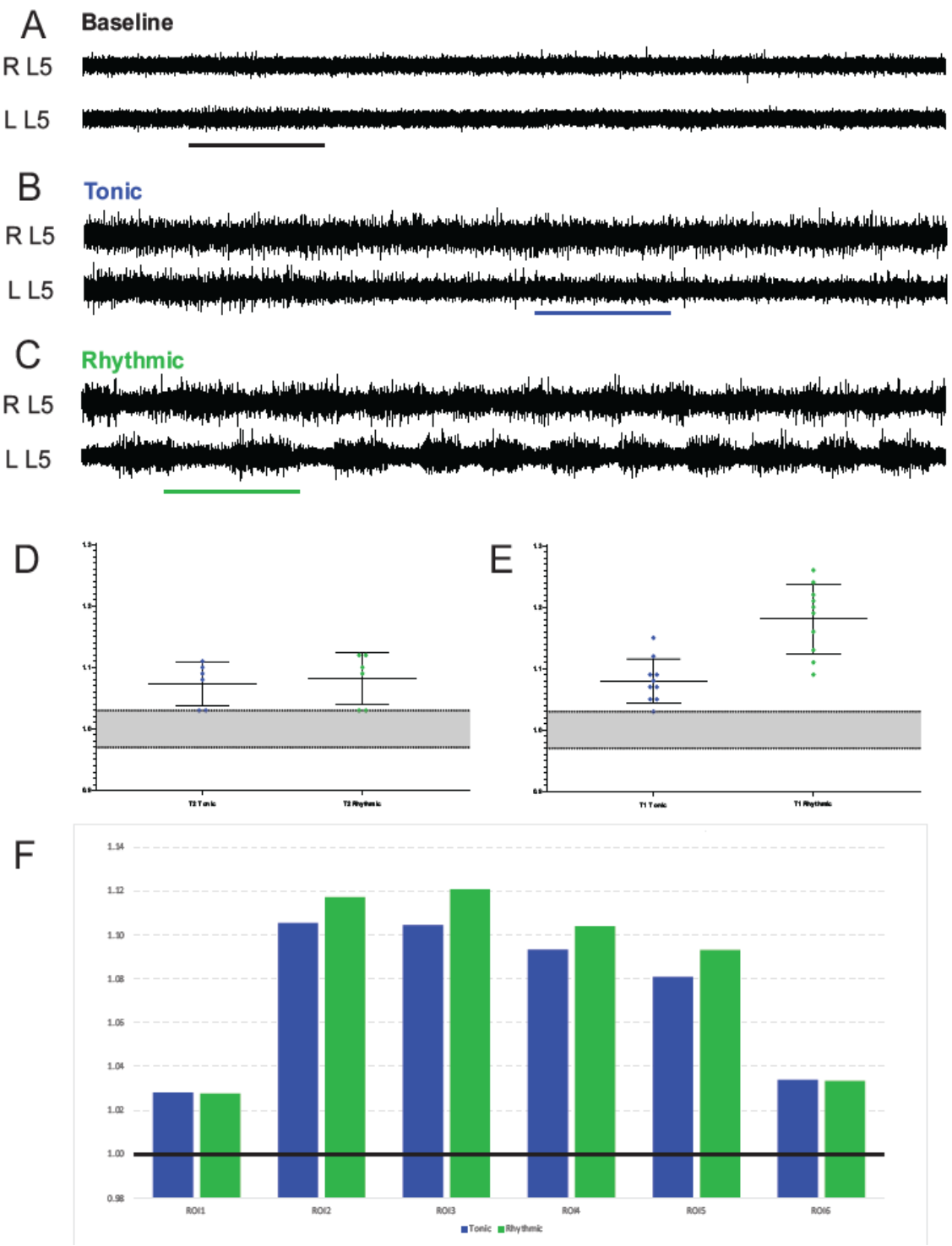

Figure 9: Thoracic SPNs at T6/T7 demonstrate increased activity exclusively in response to tonic and rhythmic lumbar VR output in some preparations. There were two trials (T1 and T2) in this preparation. ENG recording obtained during the second trial in bilateral L5 VRs at baseline (A), during tonic (B), and rhythmic (C) activity. D & E) The charts represent grouped mean with individual data points during tonic and rhythmic VR in trial 1 (10 SPNs) and trial 2 (6

SPNs). The shaded grey is the 'no intensity change' range. All SPNs recorded in the two trials demonstrated increased calcium intensity during both tonic and rhythmic VR activity. F) The bar chart displays the average changes in calcium intensity relative to baseline in the 6 recorded SPNs during tonic (blue) and rhythmic (green) VR. This suggests enhanced neuronal activation in all recorded SPNs during drug-induced motor activity (40μM 5HT, 10μM NMDA, 50μM DA); P1 mouse.

Rostrocaudal Spinal Level of Calcium Imaging	Number of Preparations	Number of SPNs with increased intensity of Calcium Response (Rhythmic VR)	Number of SPNs with decreased intensity of Calcium Response (Rhythmic VR)	Percent (%) with Increase	Percent (%) with Decrease
T4/T5	1	11/23	4/23	49	17
T6/T7	1	16/16	0/16	100	0
T7	1	3/4	0/4	75	0
T7/T8	2	5/19	3/19	26	16
T8/T9	5	5/42	10/42	12	24
T9	1	0/16	0/16	0	0
T9/T10	9	18/110	23/110	16	21
T10/T11	4	8/43	6/43	19	14
T12/T13	1	1/4	1/4	25	25

Table 4: **Summary of SPN calcium intensity changes during rhythmic ventral root discharge at different rostrocaudal thoracic levels.**

3.6 SPN Recruitment During Neurochemical-Induced Ventral Root Activity

In 12 experimental trials (n=10 mice), additional ROIs became visible in the IML during tonic and/or rhythmic lumbar locomotor activity, and these were referred to as "recruited SPNs." In 2 out of the 12 trials, drug application only evoked increased tonic VR discharge. This increased tonic VR activity was accompanied by the appearance of new SPNs (6 new ROIs) in addition to initial SPNs visualized at baseline. In other trials where drug application induced rhythmic VR activity without an intermediate tonic increase, 11 additional SPNs were also identified (3 trials). In 5/12 trials, 15 new SPNs were recruited during tonic VR discharge. These newly recruited SPNs remained active during rhythmic ventral root bursting. Finally, in the last two trials, 7 new SPNs appeared during tonic VR increase, and further recruitment (an additional 4) was observed when VR activity transitioned to rhythmic. In **Figure 10,** seven SPNs were initially identified at baseline (**Figure 10A, 10B**). However, two additional SPNs became visually apparent during tonic VR activity (**Figure 10C, 10D**) and persisted during rhythmic VR activity (**Figure 10E, 10F**).

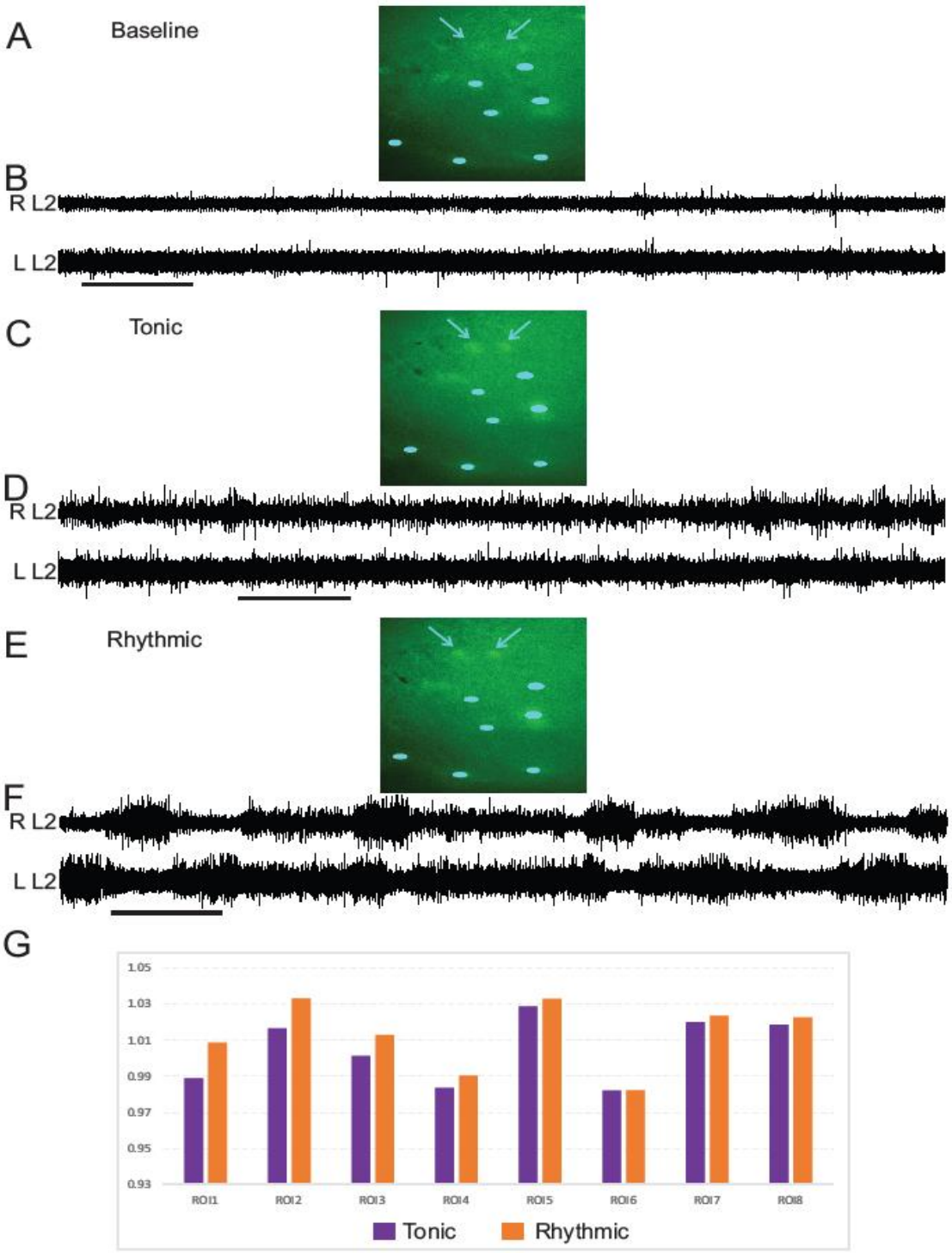

Figure 10: SPN recruitment during tonic and rhythmic VR activity. A) Masked regions represent preloaded SPNs in T9/T10 visibly present in the IML and recorded during baseline VR activity (B). Two newly recruited SPNs become visually apparent and persist in the IML (C & E) during tonic (D) and rhythmic (F) VR activity induced with 20μM 5HT, 5μM NMDA, and 50μM DA combination; P4 mouse.

3.7 Differential SPN Activity at Various Thoracic Spinal Levels

SPNs are somatotopographically arranged in the thoracolumbar spinal cord. For example, SPNs innervating the heart reside in the T1 to T6 spinal segments, whereas SPNs innervating the adrenal glands are found in T6 to T10. We, therefore, grouped and analyzed SPN activity patterns at different thoracic spinal levels. SPNs were divided into those located in the rostral (T1-T7) and caudal (T8-T13) thoracic spinal segments. We focused on SPNs that showed 3% or more change from baseline fluorescence intensities and characterized their activity patterns at different segmental levels. A total of 47 SPNs were recorded in the rostral thoracic SC during tonic VR activity. 30 SPNs (63%) demonstrated increased activity. In comparison, a decrease was seen in 8 SPNs (17%). 184 SPNs were examined in the caudal thoracic SC, with 36 and 30 SPNs demonstrating increased (20%) and decreased (16%) fluorescent intensity, respectively. Our data indicated that compared to SPNs in caudal thoracic segments, a higher proportion of SPNs in the rostral thoracic SC demonstrate an increased activity during tonic VR discharge.

This finding was consistent with our observation of an apparent segmental distribution of SPN activity during rhythmic VR activity. In particular, 35 out of 62 recorded rostral thoracic SPNs displayed increased fluorescence (56%), and 7 exhibited decreased fluorescence (11%). In the caudal thoracic segments, we observed increased activity in 32 out of 215 SPNs (15%) and a decrease in 40 SPNs (19%). Like tonic VR activity, our results showed that most SPNs characterized in the rostral thoracic spinal levels (T1-T7) exhibit increased activity during fictive locomotion. In contrast, more SPNs found in the caudal thoracic spinal segments showed decreased activity during fictive locomotion (**Figure 11**).

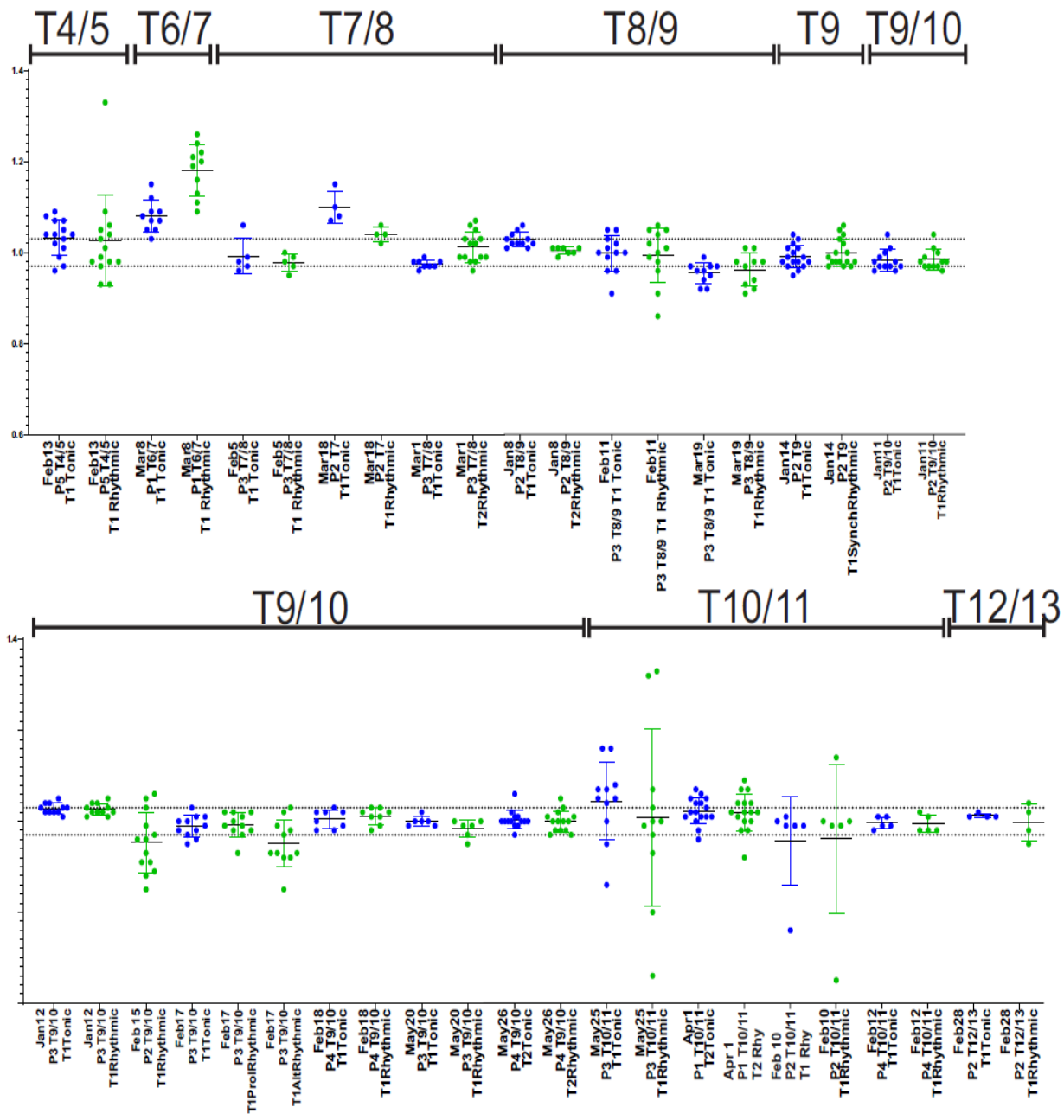

Figure 11: SPN mean calcium intensity levels at different thoracic spinal levels during drug-induced lumbar ventral root activity. A higher proportion of SPNs in the rostral thoracic segments (T4-T7) displayed increased mean calcium intensity change relative to their baseline (dotted area). Conversely, SPNs recorded in the mid and caudal thoracic spinal cord (T8-T13) demonstrated less variability from their baseline. However, note that many thoracic SPNs recorded below the T7 spinal level showed a decrease rather than an increase from baseline intensity during tonic (in blue) and rhythmic (in green) locomotor activity.

In a similar manner, **Figure 12** represents our recorded MN mean calcium intensity levels at different thoracic spinal levels during lumbar locomotor activity. Unlike SPNs, MNs appear to show less variability in their activity during lumbar locomotor activity relative to baseline. The number of preparations, recording spinal levels, and total number of SPNs, including the numbers that demonstrated increased or decreased intensity with tonic and rhythmic VR activity, are outlined in **Tables 3 and 4**, respectively.

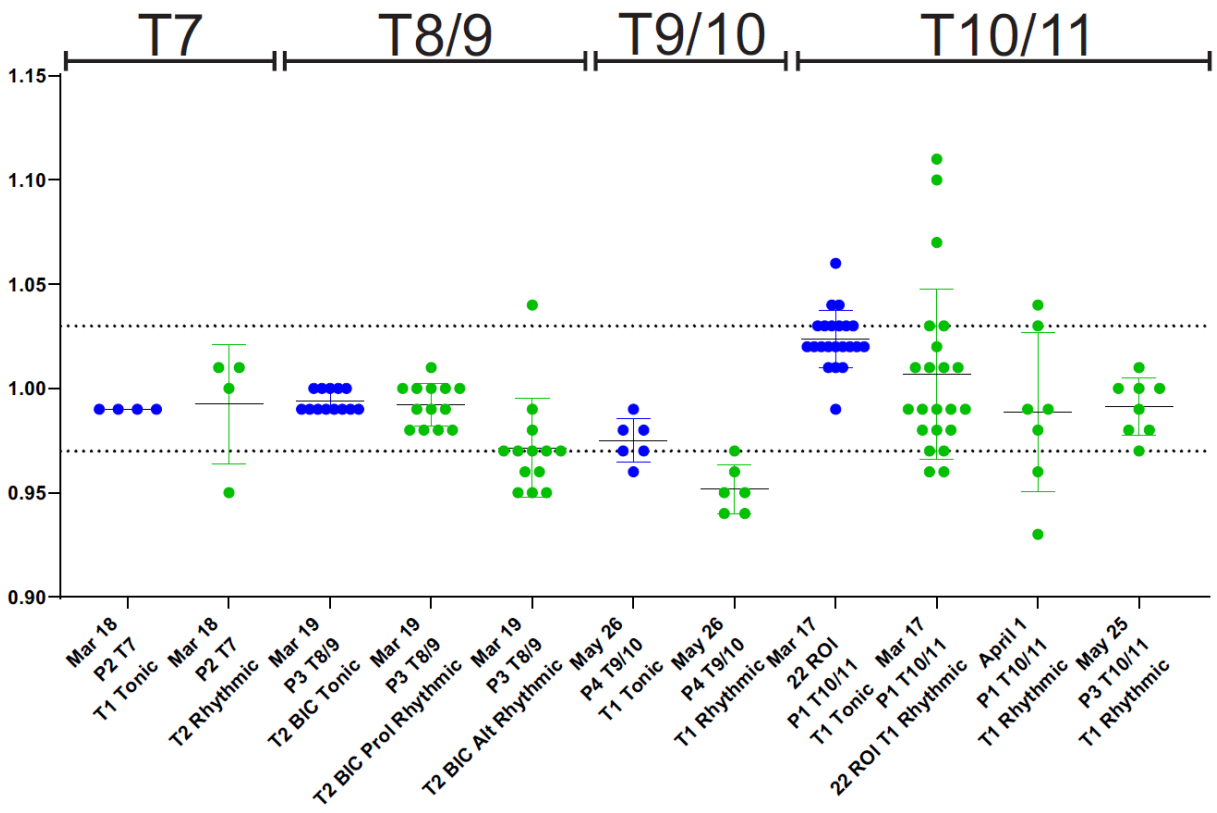

Figure 12: MN mean calcium intensity levels at different thoracic spinal levels during drug-induced lumbar ventral root activity. In contrast to SPNs, motoneurons exhibit a comparatively lower level of variability in their activity during lumbar tonic (in blue) and rhythmic (in green) ventral root activity compared to baseline.

Chapter IV: Discussion

4.1 Summary of Findings

In this study, we performed the first characterization of the activity patterns of sympathetic preganglionic neurons during drug-induced fictive locomotion in the neonatal mouse spinal cord. We showed that SPNs frequently demonstrate spontaneous calcium oscillations at baseline and greater oscillations during drug-induced rhythmic locomotor-like activity. Additionally, thoracic SPNs show increased, decreased, or no change in their mean calcium intensities relative to baseline during tonic and rhythmic VR activity. When considering individual thoracic segments, it appeared that a higher proportion of SPNs in the T1-T7 segments exhibited increased calcium intensity levels during both tonic and rhythmic VR activity. In contrast, SPNs that demonstrated decreased calcium intensity during tonic and rhythmic VR activity were often located in the caudal (T8-T13) thoracic segments. In some experiments, we also observed that additional SPNs were recruited during both tonic and rhythmic locomotor-like activity. Together, our results suggest that subpopulations of SPNs may have distinct roles during lumbar locomotor activity.

4.2 Development of Methods

To investigate whether intraspinal neurons contribute to coordinating the activity between spinal locomotor circuits and SPNs, we developed an *in vitro* spinal cord preparation to allow monitoring and recording of SPN activity during fictive locomotion. To improve the survival of the isolated spinal cord, we used neonates for this project, as has been used in other studies (Cowley and Schmidt 1994, Cowley and Schmidt 1994, Cowley and Schmidt 1997, Whelan, Bonnot et al. 2000, Jean-Xavier and Perreault 2018). Our spinal cord preparation allowed us to

visualize up to 30 neurons per optical section. Populations of labeled SPNs were identified on an oblique plane, and the changes in fluorescence (related to calcium transients) were recorded before and during drug-induced VR activity. An experimental approach similar to the one described in this study has been used to investigate descending connections from the brainstem to motoneurons and spinal interneurons thought to be involved in postural responses (Szokol and Perreault 2009). Although neuronal calcium responses can be recorded in a transverse plane without an oblique cut, as described in this study, the modification makes it possible to see neurons that would otherwise not be visible (Szokol and Perreault 2009). We have shown that our spinal cord preparation and experimental approach provide a means to identify somas of SPNs and MNs rapidly, describe their distribution across different spinal segments, and record their activity during fictive locomotion. This method can also be used to provide insights into functional connections that may exist between various neuronal populations within the spinal cord.

4.3 Spontaneous and Drug-Induced Ventral Root Motor Patterns in Neonatal Mouse Spinal Cord

Spontaneous VR activity was observed in 15 out of 26 isolated spinal cord preparations. There were variable patterns of motor output seen in the absence of neurochemicals. *In vitro,* spontaneous VR activity is rarely well coordinated or sustained, which is thought to correlate with ataxic movements frequently observed in neonatal rodents (Bonnot, Morin et al. 1998, Dalrymple, Sharples et al. 2019). This spontaneous activity was present in one or both suctioned lumbar ventral roots and consisted of intermittent short-duration rhythmic bursting. The varying

numbers of SPNs active at baseline may correlate with this spontaneous VR discharge. Upon bath application of neurochemicals, spontaneous ventral root activity transitioned to tonic or rhythmic discharge. In some trials, the appearance of rhythmic locomotor-like activity was preceded by initial tonic discharge (25/36 trials).

Our study showed that several different locomotor-like patterns could be evoked from bath application of several neurochemical cocktails. Consistent with previous studies (Whelan (Cazalets, Sqalli-Houssaini et al. 1992, Cowley and Schmidt 1994, Cazalets, Borde et al. 1995, Whelan, Bonnot et al. 2000), serotonin was the best single neurochemical to induce an alternating VR locomotor-like pattern of activity. Synchronous rhythmic discharge in bilateral extensor VRs was also observed in trials with bicuculline (an inhibitory neurotransmitter antagonist) in the bath. In our experimental series, a combination of 5HT, NMDA, and DA most reliably evoked a persistent alternating left/right rhythmic activity in the ventral roots (L2 or L5 bilaterally). However, in some preparations (n=15), 5HT/NMDA-containing cocktails failed to induce a well-organized rhythmic VR motor pattern. One possible reason may be that exogenous drug application does not mimic the timed release of neurotransmitters as expected *in vivo* (Cowley and Schmidt 1994). Similar to that seen in rats, bath application of neurochemicals to neonatal mouse spinal cord produces an unpredictable VR pattern of activity (Cowley and Schmidt 1994, Whelan, Bonnot et al. 2000). A detailed understanding of the mechanisms of drug-induced rhythmic activity would be relevant to interpret the various VR motor patterns that can be evoked in the mouse spinal cord (Whelan, Bonnot et al. 2000). As this is the first time SPN activity is characterized as it relates to rhythmic locomotor activity, we recorded SPN calcium responses during different drug-induced VR rhythmic motor patterns. Also, based on our

limited sample size, we are unable to correlate baseline spontaneous activity and the different types of VR discharge.

4.4 Generation of Rhythmic Oscillations in Thoracic SPNs at Baseline and During Drug-Induced Locomotor-Like Activity

Rhythmic discharge has been observed in neuronal populations in areas of the central nervous system (like the CPG, respiratory neurons, and subpopulations of thalamic and hippocampal neurons). The inherent rhythmogenic capability is thought to be related to the diverse functional roles of these different neural networks (Llinas 1988). Sympathetic neuronal networks frequently demonstrate spontaneous rhythmic oscillations in the *in vivo* (Allen, Adams et al. 1993, Malpas 1998) and *in vitro* preparations (Pierce, Deuchars et al. 2010). The frequencies of ongoing activity in SPNs were 0.3-5Hz in the brainstem-spinal cord preparation (Deuchars, Spyer et al. 1995) and 7.5–22 Hz in the slice preparation (Pierce, Deuchars et al. 2010). *In vivo*, the frequency band of IML oscillations was between 8 and 12 Hz (Green and Heffron 1967). This suggests that the frequency of the rhythms varies according to the preparation used or the recording conditions (Deuchars and Lall 2015) and may reflect the underlying behavioral capabilities of each preparation.

Several other studies provide supportive evidence that serotonin is an essential modulator of rhythmic SPN activity (Orer, Clement et al. 1996, Madden and Morrison 2006, Marina, Taheri et al. 2006, Pierce, Deuchars et al. 2010). Functionally, sympathetic rhythmicity is assumed to lead to improved target organ responses compared to continuous tonic activity (Pierce, Deuchars et al. 2010). It is also postulated that vasoconstrictor SPNs are more likely to demonstrate

spontaneous ongoing rhythmic activity than other SPNs (Deuchars and Lall 2015). This observed activity may be related to their responsibility of maintaining appropriate vascular basal tone.

The generation of rhythmic activity within sympathetic systems was initially thought to originate from supraspinal centers (Barman and Gebber 2000). However, SPN rhythmicity is seen in slice preparations in which descending input is removed (Deuchars 2007, Pierce, Deuchars et al. 2010). Similarly, in our whole spinal cord preparation, in which supraspinal input is removed, 26% of SPNs demonstrated rhythmic oscillations. This is comparable to the 26% reported in rat spinal cord slices (Logan, Pickering et al. 1996). Our calculated percentage is, however, less than the percentages of spontaneously active SPNs reported in adult rats *in vivo;* 38% (Marks, Stein et al. 1990) and 39% (Coote, Macleod et al. 1981) and neonatal rat brainstem-spinal cord preparation (37% in Deuchars, Spyer et al. 1995). Our demonstration of SPN rhythmicity in the whole spinal cord preparation suggests that local spinal circuits and/or SPN intrinsic membrane properties generate basal rhythmicity in SPNs without brainstem influences. In addition, whether these rhythms are related to the activation of locomotor circuitry remains unknown.

Our observation of increased amplitude of ongoing SPN oscillations during rhythmic ventral root activity may be due to a direct effect of neurochemicals on the SPNs. This is similar to the report of the increased strength of SPN spontaneous oscillations with bath application of 5HT to rat spinal cord slices (Pierce, Deuchars et al. 2010). Another possibility is that the increased strength of SPN oscillations during rhythmic VR activity may result from the increased locomotor drive from the lumbar ascending propriospinal neurons. The latter would suggest an integration between the spinal sympathetic systems with spinal locomotor circuits to provide

homeostatic support for the ongoing movement. However, further investigations are required using split bath preparation to differentiate the two possibilities.

4.5 Differential SPN Activity Patterns at Various Rostrocaudal Thoracic Levels During Tonic and Rhythmic Locomotor Activity

Various rhythmic motor patterns can be induced by exogenously applying neurochemicals to the isolated neonatal spinal cord. Despite the limitations of ventral root recordings for monitoring fictive locomotion, the rhythmic alternation between contralateral ventral roots suggests locomotor-like activity (Cowley and Schmidt 1994, Whelan, Bonnot et al. 2000). In most VR recordings, the first observation upon applying neurochemicals was the appearance of tonic activity, which was frequently followed by different types of rhythmic patterns. This finding is consistent with reports of Cowley and Schmidt (1994) and Whelan et al. (2000) in the isolated neonatal rat and mouse spinal cords, respectively. A combination of 5HT, NMDA, and DA most reliably induced rhythmic patterns in the ventral roots. Our drug combination for inducing fictive locomotion is in keeping with the report of the pharmacological condition that most consistently evokes stable locomotor activity in the neonatal mouse spinal cord (Whelan, Bonnot et al. 2000).

SPN calcium responses, which reflect neuronal activity, were recorded at baseline and during tonic and rhythmic VR activity. Our study showed that different proportions of SPNs demonstrated an increase, a decrease, or no change in mean calcium intensity levels at different thoracic spinal levels during lumbar tonic discharge and rhythmic locomotor activity. **Tables 3 and 4** show the numbers of recorded SPNs that decreased or increased their activity with the

activation of spinal locomotor circuitry. The remaining SPNs, which showed less than a 3% change from baseline fluorescence intensity, were considered to have shown no change during locomotor activity.

The wide variability in the activity of these SPNs at different thoracic levels during drug-induced locomotor activity may be due to various factors. It may be due to changes in individual SPN intrinsic properties, their expression of receptors for the drugs, their baseline activity levels, or their target tissues and particular role in maintaining homeostasis. SPN responses may also result from excitatory or inhibitory input from spinal interneurons that regulate sympathetic output. Lastly, the varied SPN responses at different thoracic spinal levels during locomotor activity may be due to other unknown factors.

Our data suggest that a higher proportion of SPNs recorded in the rostral thoracic segments (T1-T7) demonstrates an increase in their mean fluorescence intensity compared to their baseline fluorescence. In contrast, those recorded from the caudal T8-T13 segments primarily show decreased fluorescence intensities during locomotor activity. SPNs in the rostral thoracic segments are involved in the sympathetic control of targets like the heart, lungs, pupils, and salivary glands (Llewellyn-Smith and Verberne 2011, Cowley 2018). In contrast, SPNs in the caudal thoracic and upper lumbar segments innervate targets like the kidneys, bowel, and bladder in the lower body (Llewellyn-Smith and Verberne 2011, Deuchars and Lall 2015). SPNs in the caudal thoracic segments innervate targets like the kidneys, bowel, and bladder in the lower body, which would likely be inhibited or show decreased activity during ongoing rhythmic movements. The differences in proportions of rostral or caudal SPNs demonstrating an increase, or a decrease may be linked to their general organization in the spinal cord and their role during sustained movement. It may be explained by increased sympathetic activation of targets like

cardiovascular tissues and the lungs and coordinated inhibition of tissues like the intestines during movement and exercise (Cowley 2018).

It is also important to note that our observation of a wide variability of SPN activity in response to drug-induced fictive locomotion is not unusual. Similar variability has been observed in the same neuronal population responding to a stimulus. For instance, the application of neurochemicals like serotonin, norepinephrine, or dopamine to neonatal rodent spinal cord elicited both excitatory and inhibitory responses in populations of motoneurons (Neuman 1985, Takahashi and Berger 1990, Wang and Dun 1990, Muramoto, Mendelson et al. 1996, Sharples, Burma et al. 2020).

4.6 Additional Thoracic SPNs Can be Recruited During Lumbar Locomotor Activity

Our data showed the appearance of additional SPN activity in the intermediolateral nucleus during tonic discharge or rhythmic locomotor activity. In addition to the appearance of new SPNs in some of our trials, those present at baseline showed increased, decreased, or no change in mean calcium intensity during fictive locomotion. New SPNs becoming visible during locomotor activity suggest the recruitment of the sympathetic neurons to support the ongoing movement. The idea of sympathetic recruitment during sustained movement and exercise has also been demonstrated in animal (Kaufman, Longhurst et al. 1983) and human (Iellamo (Iellamo, Legramante et al. 2002) studies. As already described in our study background, spinalized animals (rats and monkeys) that undergo lumbar electrical stimulation show improvement in motor and some autonomic functions like blood pressure (Squair, Gautier et al. 2021). Similar reports have been documented in humans with spinal cord injury who undergo

spinal electrical stimulation targeted to improve voluntary movement (Harkema, Legg Ditterline et al. 2018, Phillips, Squair et al. 2018, Darrow, Balser et al. 2019, Legg Ditterline, Aslan et al. 2021). The recovery of autonomic functions with activation of lumbar locomotor circuitry and our observation of SPN recruitment during rhythmic locomotor activity is consistent with the concept of ascending locomotor drive providing input to the spinal sympathetic network. It is pertinent to note that coordinated recruitment of the sympathetic neurons is necessary to maintain homeostasis and to provide metabolic substrates to active body tissues during sustained movement.

4.7 Limitations and Future Directions

One limitation of our experiments was that neurochemicals were applied directly to the whole spinal cord bath. Although SPNs demonstrated various responses during lumbar locomotor activity, we are not sure that the locomotor circuitry strictly drives these responses or is not a result of a direct effect of drugs on the SPNs. To determine whether SPN responses are indeed altered during fictive locomotion, we will need to perform these experiments in a split bath. The split bath will create a barrier in the recording chamber to separate the thoracic from the lumbar spinal cord. Application of neurochemicals will then be restricted to the lumbar spinal cord to activate only the locomotor neural circuitry while recording SPN responses in the thoracic spinal segments. This work is presently ongoing in our laboratory.

Another limitation of our study was the sampling frequency of the SPNs. Most of our SPN activities were sampled at 7.5 Hz. The decision to use the lower sampling frequency for recording most SPN activity was informed by a balance of two factors: concerns about

phototoxicity for our long recording sessions (approx. 75mins total time per session) and the frequency of SPN oscillations reported in the literature. To minimize photobleaching, parameters like low epi-illumination intensity and low sampling frequency can reduce neuronal exposure time and phototoxicity (Szokol and Perreault 2009). Regarding firing rate, Deuchars and colleagues documented that a third of SPNs displaying ongoing activity fired at around 1-2 Hz, and the remaining were in the range of 0.2-5 Hz in the brainstem-spinal cord preparation (Deuchars, Spyer et al. 1995). Pierce et al. (2010), however, reported that the frequency of IML oscillations can range from 7.5 to 22 Hz. They also noted that the range of frequencies of spontaneous and 5HT-induced rhythms was not significantly different. With most of our SPNs sampled at 7.5 Hz, it is possible that the activity of some SPNs oscillating at higher frequencies would have been missed in our study, resulting in a loss of information and incorrect interpretation of the data. In future experiments, SPNs will be sampled at higher frequencies and in shorter recording sessions to allow us to capture the relevant information at each timescale and thus obtain a complete picture of neuronal activity.

The other consideration concerns our sample size and bias in recording thoracic levels. Most of the SPN recordings were obtained from thoracic spinal levels T8-T10. Based on PRV labeling, these segments provide diverse SPN projections to many internal body tissues and organs and so would be ideal for SPN activity characterization during fictive locomotion. It is, however, important to note that due to the small and delicate nature of rostral thoracic VRs, they are more challenging to see and dissect and are easily lost during dissection. This makes it difficult to retrogradely label the SPNs, especially at T1-T4 spinal levels. However, to determine whether there is an actual differential SPN activity pattern at various thoracic levels, there is a need to equally assess SPN responses in all thoracic segments during VR activity. In future

experiments, we will use transgenic mouse lines expressing genetically encoded calcium indicators in cholinergic neurons to remedy this technical challenge. Because SPNs are cholinergic neurons, the protein will be incorporated and, like the CGDA dye, will fluoresce in response to neuronal activity. The gCaMP mouse models will eliminate the need to backfill the SPNs with a calcium dye, decrease the time for spinal cord preparation and facilitate our visualization and systematic characterization of SPN activity during locomotion at all thoracic spinal levels.

Chapter V: Conclusions

This is the first time SPN activity has been characterized during drug-induced lumbar locomotor activity.

Characterization of SPN activity revealed that:

i. SPNs can show rhythmic calcium oscillations at baseline.
ii. SPNs can demonstrate greater oscillations during rhythmic VR activity.
iii. Additional thoracic SPNs are recruited during lumbar locomotor activity.
iv. SPNs may show increases, decreases, or no change in their mean calcium intensities during lumbar locomotor activity.
v. There may be differences in SPN activity patterns at different rostrocaudal thoracic levels during rhythmic locomotor activity.

These findings suggest distinct roles for different SPN subpopulations during lumbar locomotor activity. By revealing new insights, the results of this study improve our understanding of intraspinal functional connectivity between locomotor and sympathetic functions. While many questions remain, there is a continued need to explore the capacity of the spinal cord to coordinate these functions to optimize strategies like epidural stimulation for motor and autonomic recovery in people with SCI.

References

Adler, E. S., J. H. Hollis, I. J. Clarke, D. R. Grattan and B. J. Oldfield (2012). "Neurochemical characterization and sexual dimorphism of projections from the brain to abdominal and subcutaneous white adipose tissue in the rat." J Neurosci **32**(45): 15913-15921.

Allen, A. M., J. M. Adams and P. G. Guyenet (1993). "Role of the spinal cord in generating the 2- to 6-Hz rhythm in rat sympathetic outflow." Am J Physiol **264**(5 Pt 2): R938-945.

Anderson, K. D. (2004). "Targeting recovery: priorities of the spinal cord-injured population." J Neurotrauma **21**(10): 1371-1383.

Angeli, C. A., V. R. Edgerton, Y. P. Gerasimenko and S. J. Harkema (2014). "Altering spinal cord excitability enables voluntary movements after chronic complete paralysis in humans." Brain **137**(Pt 5): 1394-1409.

Anson, C. A. and C. Shepherd (1996). "Incidence of secondary complications in spinal cord injury." Int J Rehabil Res **19**(1): 55-66.

Armstrong, D. M. (1986). "Supraspinal contributions to the initiation and control of locomotion in the cat." Progress in Neurobiology **26**: 273-361.

Armstrong, K. A. E., M. Nazzal, X. Chen, U. Slawinska, L. M. Jordan, K. C. Cowley and K. Stecina (2023). "Chemogenetic and optogenetic activation of descending serotonergic neurons reveals role in hindlimb locomotor and blood pressure control." Front Neural Circuits.

Ballion, B., D. Morin and D. Viala (2001). "Forelimb locomotor generators and quadrupedal locomotion in the neonatal rat." Eur J Neurosci **14**(10): 1727-1738.

Bamshad, M., V. T. Aoki, M. G. Adkison, W. S. Warren and T. J. Bartness (1998). "Central nervous system origins of the sympathetic nervous system outflow to white adipose tissue." Am J Physiol **275**(1 Pt 2): R291-299.

Bamshad, M., C. K. Song and T. J. Bartness (1999). "CNS origins of the sympathetic nervous system outflow to brown adipose tissue." Am J Physiol **276**(6 Pt 2): R1569-1578.

Barajon, I., J. P. Gossard and H. Hultborn (1992). "Induction of fos expression by activity in the spinal rhythm generator for scratching." Brain Res **588**(1): 168-172.

Barbeau, H. and S. Rossignol (1991). "Initiation and modulation of the locomotor pattern in the adult chronic spinal cat by noradrenergic, serotonergic and dopaminergic drugs." Brain Research **546**: 250-260.

Barman, S. M. and G. L. Gebber (2000). ""Rapid" rhythmic discharges of sympathetic nerves: sources, mechanisms of generation, and physiological relevance." J Biol Rhythms **15**(5): 365-379.

Berlowitz, D. J., B. Wadsworth and J. Ross (2016). "Respiratory problems and management in people with spinal cord injury." Breathe (Sheff) **12**(4): 328-340.

Bigelow, W. G. (1958). "Hypothermia." Surgery **43**(4): 683-687.

Bloom, O., J. M. Wecht, B. E. Legg Ditterline, S. Wang, A. V. Ovechkin, C. A. Angeli, A. A. Arcese and S. J. Harkema (2020). "Prolonged Targeted Cardiovascular Epidural Stimulation Improves Immunological Molecular Profile: A Case Report in Chronic Severe Spinal Cord Injury." Front Syst Neurosci **14**: 571011.

Bonnot, A., D. Morin and D. Viala (1998). "Genesis of spontaneous rhythmic motor patterns in the lumbosacral spinal cord of neonate mouse." **108**(1-2): 89-99.

Boulain, M., I. Khsime, M. Sourioux, M. Thoby-Brisson, G. Barrière, J. Simmers, D. Morin and L. Juvin (2021). "Synergistic interaction between sensory inputs and propriospinal signalling underlying quadrupedal locomotion." J Physiol **599**(19): 4477-4496.

Brustein, E. and S. Rossignol (1998). "Recovery of locomotion after ventral and ventrolateral spinal lesions in the cat. I. Deficits and adaptive mechanisms." J Neurophysiol **80**(3): 1245-1267.

Cabot, J. B. (1990). Sympathetic preganglionic neurons: Cytoarchitecture, ultrastructure and biophysical properties. Central regulation of autonomic functions. A. D. Loewy and K. M. Spyer. New York, Oxford University Press**:** 44 - 67.

Cabot, J. B., V. Alessi, J. Carroll and M. Ligorio (1994). "Spinal cord lamina V and lamina VII interneuronal projections to sympathetic preganglionic neurons." J Comp Neurol **347**(4): 515-530.

Caggiano, V., R. Leiras, H. Goñi-Erro, D. Masini, C. Bellardita, J. Bouvier, V. Caldeira, G. Fisone and O. Kiehn (2018). "Midbrain circuits that set locomotor speed and gait selection." Nature **553**(7689): 455-460.

Capogrosso, M., N. Wenger, S. Raspopovic, P. Musienko, J. Beauparlant, L. Bassi Luciani, G. Courtine and S. Micera (2013). "A computational model for epidural electrical stimulation of spinal sensorimotor circuits." J Neurosci **33**(49): 19326-19340.

Cazalets, J. R., M. Borde and F. Clarac (1995). "Localization and organization of the central pattern generator for hindlimb locomotion in newborn rat." Journal of Neuroscience **15**(7): 4943-4951.

Cazalets, J. R., Y. Sqalli-Houssaini and F. Clarac (1992). "Activation of the central pattern generators for locomotion by serotonin and excitatory amino acids in neonatal rat." Journal of Physiology **455**: 187-204.

Chen, Y., Y. Tang, L. C. Vogel and M. J. Devivo (2013). "Causes of spinal cord injury." Top Spinal Cord Inj Rehabil **19**(1): 1-8.

Chopek, J. W., F. Nascimento, M. Beato, R. M. Brownstone and Y. Zhang (2018). "Sub-populations of Spinal V3 Interneurons Form Focal Modules of Layered Pre-motor Microcircuits." Cell Rep **25**(1): 146-156 e143.

Chopek, J. W., Y. Zhang and R. M. Brownstone (2021). "Intrinsic brainstem circuits comprised of Chx10-expressing neurons contribute to reticulospinal output in mice." J Neurophysiol **126**(6): 1978-1990.

Cina, C. and S. Hochman (2000). "Diffuse distribution of sulforhodamine-labeled neurons during serotonin-evoked locomotion in the neonatal rat thoracolumbar spinal cord." J Comp Neurol **423**(4): 590-602.

Clarke, H. A., G. A. Dekaban and L. C. Weaver (1998). "Identification of lamina V and VII interneurons presynaptic to adrenal sympathetic preganglionic neurons in rats using a recombinant herpes simplex virus type 1." Neuroscience **85**(3): 863-872.

Cohen, A. H. and P. Wallen (1980). "The neuronal correlate of locomotion in fish. "Fictive Swimming" induced in an in vitro preparation of the lamprey spinal cord." Experimental Brain Research **41**: 11-18.

Coote, J. H., V. H. Macleod, S. Fleetwood-Walker and M. P. Gilbey (1981). "The response of individual sympathetic preganglionic neurones to microelectrophoretically applied endogenous monoamines." Brain Res **215**(1-2): 135-145.

Courtine, G., Y. Gerasimenko, R. van den Brand, A. Yew, P. Musienko, H. Zhong, B. Song, Y. Ao, R. M. Ichiyama, I. Lavrov, R. R. Roy, M. V. Sofroniew and V. R. Edgerton (2009). "Transformation of nonfunctional spinal circuits into functional states after the loss of brain input." Nat Neurosci **12**(10): 1333-1342.

Cowley, K. C. (2018). "A new conceptual framework for the integrated neural control of locomotor and sympathetic function: implications for exercise after spinal cord injury." Appl Physiol Nutr Metab **43**(11): 1140-1150.

Cowley, K. C. and B. J. Schmidt (1994). "A comparison of motor patterns induced by N-methyl-D-aspartate, acetylcholine and serotonin in the in vitro neonatal rat spinal cord." Neuroscience Letters **171**: 147-150.

Cowley, K. C. and B. J. Schmidt (1994). "Some limitations of ventral root recordings for monitoring locomotion in the in vitro neonatal rat spinal cord preparation." Neuroscience Letters **171**: 142-146.

Cowley, K. C. and B. J. Schmidt (1997). "Regional distribution of the locomotor pattern-generating network in the neonatal rat spinal cord." Journal of Neurophysiology **77**: 247-259.

Cowley, K. C., E. Zaporozhets, R. A. Joundi and B. J. Schmidt (2009). "Contribution of commissural projections to bulbospinal activation of locomotion in the in vitro neonatal rat spinal cord." J Neurophysiol **101**(3): 1171-1178.

Cowley, K. C., E. Zaporozhets, J. N. Maclean and B. J. Schmidt (2005). "Is NMDA Receptor Activation Essential for the Production of Locomotor-Like Activity in the Neonatal Rat Spinal Cord?" J Neurophysiol **94**(6): 3805-3814.

Cowley, K. C., E. Zaporozhets and B. J. Schmidt (2008). "Propriospinal neurons are sufficient for bulbospinal transmission of the locomotor command signal in the neonatal rat spinal cord." J Physiol **586**(6): 1623-1635.

Cowley, K. C., E. Zaporozhets and B. J. Schmidt (2010). "Propriospinal transmission of the locomotor command signal in the neonatal rat." Ann N Y Acad Sci **1198**: 42-53.

Crane, D. A., J. W. Little and S. P. Burns (2011). "Weight gain following spinal cord injury: a pilot study." J Spinal Cord Med **34**(2): 227-232.

Creasey, G. H. and M. D. Craggs (2012). "Functional electrical stimulation for bladder, bowel, and sexual function." Handb Clin Neurol **109**: 247-257.

Dalrymple, A. N., S. A. Sharples, N. Osachoff, A. P. Lognon and P. J. Whelan (2019). "A supervised machine learning approach to characterize spinal network function." J Neurophysiol **121**(6): 2001-2012.

Darrow, D., D. Balser, T. I. Netoff, A. Krassioukov, A. Phillips, A. Parr and U. Samadani (2019). "Epidural Spinal Cord Stimulation Facilitates Immediate Restoration of Dormant Motor and Autonomic Supraspinal Pathways after Chronic Neurologically Complete Spinal Cord Injury." J Neurotrauma **36**(15): 2325-2336.

de Groot, S., M. W. Post, K. Postma, T. A. Sluis and L. H. van der Woude (2010). "Prospective analysis of body mass index during and up to 5 years after discharge from inpatient spinal cord injury rehabilitation." J Rehabil Med **42**(10): 922-928.

Delcomyn, F. (1980). "Neural basis of rhythmic behavior in animals." Science **210**: 492-498.

Deliagina, T. G., G. N. Orlovskii and G. A. Pavlova (1983). "The capacity for generation of rhythmic oscillations is distributed in the lumbosacral spinal cord of the cat." Experimental Brain Research **53**: 81-90.

Deuchars, S. A. (2007). "Multi-tasking in the spinal cord - do 'sympathetic' interneurones work harder than we give them credit for?" Journal of Physiology-London **580**(3): 723-729.

Deuchars, S. A. and V. K. Lall (2015). "Sympathetic Preganglionic Neurons: Properties and Inputs." Comprehensive Physiology **5**(2): 829-869.

Deuchars, S. A., C. J. Milligan, R. L. Stornetta and J. Deuchars (2005). "GABAergic neurons in the central region of the spinal cord: A novel substrate for sympathetic inhibition." Journal of Neuroscience **25**(5): 1063-1070.

Deuchars, S. A., K. M. Spyer, P. A. Brooks and M. P. Gilbey (1995). "A Study of Sympathetic Preganglionic Neuronal-Activity in a Neonatal Rat Brain-Stem-Spinal Cord Preparation." Journal of the Autonomic Nervous System **52**(1): 51-63.

Drew, T. (1991). "Functional organization within the medullary reticular formation of the intact unanesthetized cat. III. Microstimulation during locomotion." J Neurophysiol **66**(3): 919-938.

Drew, T. and S. Rossignol (1984). "Phase-dependent responses evoked in limb muscles by stimulation of medullary reticular formation during locomotion in thalamic cats." J Neurophysiol **52**(4): 653-675.

Duckworth, W. C., P. Jallepalli and S. S. Solomon (1983). "Glucose intolerance in spinal cord injury." Archives of Physical Medicine and Rehabilitation **64**(3): 107-110.

Duckworth, W. C., S. S. Solomon, P. Jallepalli, C. Heckemeyer, J. Finnern and A. Powers (1980). "Glucose intolerance due to insulin resistance in patients with spinal cord injuries." Diabetes **29**(11): 906-910.

Dun, N. J. and N. Mo (1989). "Inhibitory postsynaptic potentials in neonatal rat sympathetic preganglionic neurones in vitro." J Physiol **410**: 267-281.

Edgerton, V. R. and S. Harkema (2011). "Epidural stimulation of the spinal cord in spinal cord injury: current status and future challenges." Expert Rev Neurother **11**(10): 1351-1353.

Eidelberg, E. (1981). "Consequences of spinal cord lesions upon motor function, with special reference to locomotor activity." Prog Neurobiol **17**(3): 185-202.

Eldahan, K. C. and A. G. Rabchevsky (2018). "Autonomic dysreflexia after spinal cord injury: Systemic pathophysiology and methods of management." Auton Neurosci **209**: 59-70.

Eldridge, F. L., D. E. Millhorn and T. G. Waldrop (1981). "Exercise hyperpnea and locomotion: parallel activation from the hypothalamus." Science **211**(4484): 844-846.

Etlin, A., D. Blivis, M. Ben-Zwi and A. Lev-Tov (2010). "Long and short multifunicular projections of sacral neurons are activated by sensory input to produce locomotor activity in the absence of supraspinal control." J Neurosci **30**(31): 10324-10336.

Ferreira-Pinto, M. J., H. Kanodia, A. Falasconi, M. Sigrist, M. S. Esposito and S. Arber (2021). "Functional diversity for body actions in the mesencephalic locomotor region." Cell **184**(17): 4564-4578.e4518.

Finnerup, N. B. (2017). "Neuropathic pain and spasticity: intricate consequences of spinal cord injury." Spinal Cord **55**(12): 1046-1050.

Flett, S., J. Garcia and K. C. Cowley (2022). "Spinal electrical stimulation to improve sympathetic autonomic functions needed for movement and exercise after spinal cord injury: a scoping clinical review." J Neurophysiol **128**(3): 649-670.

Flynn, J. R., B. A. Graham, M. P. Galea and R. J. Callister (2011). "The role of propriospinal interneurons in recovery from spinal cord injury." Neuropharmacology.

Frigon, A. (2017). "The neural control of interlimb coordination during mammalian locomotion." J Neurophysiol **117**(6): 2224-2241.

Frotzler, A., B. Cheikh-Sarraf, M. Pourtehrani, J. Krebs and K. Lippuner (2015). "Long-bone fractures in persons with spinal cord injury." Spinal Cord **53**: 701.

Furlan, J. C. and M. G. Fehlings (2008). "Cardiovascular complications after acute spinal cord injury: pathophysiology, diagnosis, and management." Neurosurg Focus **25**(5): E13.

Gad, P., J. Choe, M. S. Nandra, H. Zhong, R. R. Roy, Y. C. Tai and V. R. Edgerton (2013). "Development of a multi-electrode array for spinal cord epidural stimulation to facilitate stepping and standing after a complete spinal cord injury in adult rats." J Neuroeng Rehabil **10**(1): 2.

Garcia-Arguello, L. Y., J. C. O'Horo, A. Farrell, R. Blakney, M. R. Sohail, C. T. Evans and N. Safdar (2017). "Infections in the spinal cord-injured population: a systematic review." Spinal Cord **55**(6): 526-534.

Garcia-Rill, E. and R. D. Skinner (1987). "The mesencephalic locomotor region. II. Projections to reticulospinal neurons." Brain Research **411**: 13-20.

Garland, D. E., C. A. Stewart, R. H. Adkins, S. S. Hu, C. Rosen, F. J. Liotta and D. A. Weinstein (1992). "Osteoporosis after spinal cord injury." J Orthop Res **10**(3): 371-378.

Garshick, E., A. Kelley, S. A. Cohen, A. Garrison, C. G. Tun, D. Gagnon and R. Brown (2005). "A prospective assessment of mortality in chronic spinal cord injury." Spinal Cord **43**(7): 408-416.

Gladwell, S. J. and J. H. Coote (1999). "Inhibitory and indirect excitatory effects of dopamine on sympathetic preganglionic neurones in the neonatal rat spinal cord in vitro." Brain Res **818**(2): 397-407.

Goulding, M. (2009). "Circuits controlling vertebrate locomotion: moving in a new direction." Nat Rev Neurosci **10**(7): 507-518.

Graham Brown, T. (1911). "The intrinsic factors in the act of progression in the mammal." Journal of Physiology: 308-319.

Graham Brown, T. (1914). "On the nature of the fundamental activity of the nervous centres; together with an analysis of the conditioning of rhythmic activity in progression, and a theory of the evolution of function in the nervous system." Journal of Physiology **48**: 18-46.

Green, J. H. and P. F. Heffron (1967). "Observations on the origin and genesis of a rapid sympathetic rhythm." Arch Int Pharmacodyn Ther **169**(2): 403-411.

Griener, A., J. Dyck and S. Gosgnach (2013). "Regional distribution of putative rhythm-generating and pattern-forming components of the mammalian locomotor CPG." Neuroscience **250**: 644-650.

Grillner, S. (1974). "On the generation of locomotion in the spinal dogfish." Experimental Brain Research **20**: 459-470.

Grillner, S. (1975). "Locomotion in vertebrates: central mechanisms and reflex interaction." Physiological Reviews **55(2)**: 247-304.

Hachem, L. D., C. S. Ahuja and M. G. Fehlings (2017). "Assessment and management of acute spinal cord injury: From point of injury to rehabilitation." J Spinal Cord Med **40**(6): 665-675.

Hagen, E. M., S. Faerestrand, J. M. Hoff, T. Rekand and M. Gronning (2011). "Cardiovascular and urological dysfunction in spinal cord injury." Acta Neurol Scand Suppl(191): 71-78.

Hagen, E. M., T. Rekand, M. Gronning and S. Faerestrand (2012). "Cardiovascular complications of spinal cord injury." Tidsskr Nor Laegeforen **132**(9): 1115-1120.

Haque, F. and S. Gosgnach (2019). "Mapping Connectivity Amongst Interneuronal Components of the Locomotor CPG." Front Cell Neurosci **13**: 443.

Harkema, S. J., B. Legg Ditterline, S. Wang, S. Aslan, C. A. Angeli, A. Ovechkin and G. A. Hirsch (2018). "Epidural Spinal Cord Stimulation Training and Sustained Recovery of Cardiovascular Function in Individuals With Chronic Cervical Spinal Cord Injury." JAMA Neurol **75**(12): 1569-1571.

Harkema, S. J., S. Wang, C. A. Angeli, Y. Chen, M. Boakye, B. Ugiliweneza and G. A. Hirsch (2018). "Normalization of Blood Pressure With Spinal Cord Epidural Stimulation After Severe Spinal Cord Injury." Front Hum Neurosci **12**: 83.

Henke, A. M., Z. J. Billington and D. R. Gater (2022). "Autonomic Dysfunction and Management after Spinal Cord Injury: A Narrative Review." J Pers Med **12**(7).

Herman, R., J. He, S. D'Luzansky, W. Willis and S. Dilli (2002). "Spinal cord stimulation facilitates functional walking in a chronic, incomplete spinal cord injured." Spinal Cord **40**(2): 65-68.

Ho, S. and M. J. O'Donovan (1993). "Regionalization and intersegmental coordination of rhythm-generating networks in the spinal cord of the chick embryo." Journal of Neuroscience **13(4)**: 1354-1371.

Holstege, J. C. and H. G. Kuypers (1987). "Brainstem projections to spinal motoneurons: an update." Neuroscience **23**(3): 809-821.

Hornung, J. P. (2003). "The human raphe nuclei and the serotonergic system." J Chem Neuroanat **26**(4): 331-343.

Hubscher, C. H., A. N. Herrity, C. S. Williams, L. R. Montgomery, A. M. Willhite, C. A. Angeli and S. J. Harkema (2018). "Improvements in bladder, bowel and sexual outcomes following task-specific locomotor training in human spinal cord injury." PLoS One **13**(1): e0190998.

Iellamo, F., J. M. Legramante, F. Pigozzi, A. Spataro, G. Norbiato, D. Lucini and M. Pagani (2002). "Conversion from vagal to sympathetic predominance with strenuous training in high-performance world class athletes." Circulation **105**(23): 2719-2724.

Inokuchi, H., M. Yoshimura, C. Polosa and S. Nishi (1992). "Adrenergic receptors (alpha 1 and alpha 2) modulate different potassium conductances in sympathetic preganglionic neurons." Can J Physiol Pharmacol **70 Suppl**: S92-97.

Jaja, B. N. R., F. Jiang, J. H. Badhiwala, R. Schär, S. Kurpad, R. G. Grossman, J. S. Harrop, J. D. Guest, E. G. Toups, C. I. Shaffrey, B. Aarabi, M. Boakye, M. G. Fehlings and J. R. Wilson (2019). "Association of Pneumonia, Wound Infection, and Sepsis with Clinical Outcomes after Acute Traumatic Spinal Cord Injury." J Neurotrauma **36**(21): 3044-3050.

Jean-Xavier, C. and M. C. Perreault (2018). "Influence of Brain Stem on Axial and Hindlimb Spinal Locomotor Rhythm Generating Circuits of the Neonatal Mouse." Front Neurosci **12**: 53.

Jiang, Z., K. P. Carlin and R. M. Brownstone (1999). "An in vitro functionally mature mouse spinal cord preparation for the study of spinal motor networks." Brain Res **816**(2): 493-499.

Jordan, L. M. (1991). Brainstem and spinal cord mechanisms for the initation of locomotion. Neurobiological Basis of Human locomotion. M. Shimamura, S. Grillner and R. Edgerton. Tokyo, Japan Scientific Societies Press**:** 3-20.

Jordan, L. M. (1998). "Initiation of locomotion in mammals." Ann N Y Acad Sci **860**: 83-93.

Jordan, L. M., J. Liu, P. B. Hedlund, T. Akay and K. G. Pearson (2008). "Descending command systems for the initiation of locomotion in mammals." Brain Res Rev **57**(1): 183-191.

Joshi, S., M. A. Levatte, G. A. Dekaban and L. C. Weaver (1995). "Identification of spinal interneurons antecedent to adrenal sympathetic preganglionic neurons using trans-synaptic transport of herpes simplex virus type 1." Neuroscience **65**(3): 893-903.

Josset, N., M. Roussel, M. Lemieux, D. Lafrance-Zoubga, A. Rastqar and F. Bretzner (2018). "Distinct Contributions of Mesencephalic Locomotor Region Nuclei to Locomotor Control in the Freely Behaving Mouse." Curr Biol **28**(6): 884-901.e883.

Juvin, L., J. P. Le Gal, J. Simmers and D. Morin (2012). "Cervicolumbar coordination in mammalian quadrupedal locomotion: role of spinal thoracic circuitry and limb sensory inputs." J Neurosci **32**(3): 953-965.

Juvin, L., J. Simmers and D. Morin (2005). "Propriospinal circuitry underlying interlimb coordination in mammalian quadrupedal locomotion." J Neurosci **25**(25): 6025-6035.

Kahn, J. A. and A. Roberts (1982). "Experiments on the central pattern generator for swimming in amphibian embryos." Philisophical Transactions of the Royal Society of London.Series B: Biological Sciences **296**: 229-243.

Kathe, C., M. A. Skinnider, T. H. Hutson, N. Regazzi, M. Gautier, R. Demesmaeker, S. Komi, S. Ceto, N. D. James, N. Cho, L. Baud, K. Galan, K. J. E. Matson, A. Rowald, K. Kim, R. Wang, K. Minassian, J. O. Prior, L. Asboth, Q. Barraud, S. P. Lacour, A. J. Levine, F. Wagner, J. Bloch, J. W. Squair and G. Courtine (2022). "The neurons that restore walking after paralysis." Nature **611**(7936): 540-547.

Kaufman, M. P., J. C. Longhurst, K. J. Rybicki, J. H. Wallach and J. H. Mitchell (1983). "Effects of static muscular contraction on impulse activity of groups III and IV afferents in cats." J Appl Physiol Respir Environ Exerc Physiol **55**(1 Pt 1): 105-112.

Kettunen, P. (2012). "Calcium imaging in the zebrafish." Adv Exp Med Biol **740**: 1039-1071.

Kiehn, O. (2016). "Decoding the organization of spinal circuits that control locomotion." Nat Rev Neurosci **17**(4): 224-238.

Kiehn, O. and S. J. Butt (2003). "Physiological, anatomical and genetic identification of CPG neurons in the developing mammalian spinal cord." Prog Neurobiol **70**(4): 347-361.

Kiehn, O., H. Hultborn and B. A. Conway (1992). "Spinal locomotor activity in acutely spinalized cats induced by intrathecal application of noradrenaline." Neurosci Lett **143**(1-2): 243-246.

Kiehn, O. and O. Kjaerulff (1996). "Spatiotemporal characteristics of 5-HT and dopamine-induced rhythmic hindlimb activity in the in vitro neonatal rat." Journal of Neurophysiology **75**(4): 1472-1482.

Kjaerulff, O. and O. Kiehn (1996). "Distribution of networks generating and coordinating locomotor activity in the neonatal rat spinal cord in vitro: A lesion study." Journal of Neuroscience **16**(18): 5777-5794.

Koba, S., N. Kumada, E. Narai, N. Kataoka, K. Nakamura and T. Watanabe (2022). "A brainstem monosynaptic excitatory pathway that drives locomotor activities and sympathetic cardiovascular responses." Nat Commun **13**(1): 5079.

Kremer, E. and A. Lev-Tov (1997). "Localization of the spinal network associated with generation of hindlimb locomotion in the neonatal rat and organization of its transverse coupling system." J Neurophysiol **77**(3): 1155-1170.

Krogh, A. and J. Lindhard (1913). "The regulation of respiration and circulation during the initial stages of muscular work." J Physiol **47**(1-2): 112-136.

Krueger, H., V. K. Noonan, L. M. Trenaman, P. Joshi and C. S. Rivers (2013). "The economic burden of traumatic spinal cord injury in Canada." Chronic Dis Inj Can **33**(3): 113-122.

Krupp, J. and P. Feltz (1995). "Excitatory postsynaptic currents and glutamate receptors in neonatal rat sympathetic preganglionic neurons in vitro." J Neurophysiol **73**(4): 1503-1512.

Laliberte, A. M., S. Goltash, N. R. Lalonde and T. V. Bui (2019). "Propriospinal Neurons: Essential Elements of Locomotor Control in the Intact and Possibly the Injured Spinal Cord." Front Cell Neurosci **13**: 512.

Lavela, S. L., F. M. Weaver, B. Goldstein, K. Chen, S. Miskevics, S. Rajan and D. R. Gater, Jr. (2006). "Diabetes mellitus in individuals with spinal cord injury or disorder." J Spinal Cord Med **29**(4): 387-395.

Lee, B. B., R. A. Cripps, M. Fitzharris and P. C. Wing (2014). "The global map for traumatic spinal cord injury epidemiology: update 2011, global incidence rate." Spinal Cord **52**(2): 110-116.

Legg Ditterline, B. E., S. C. Aslan, S. Wang, B. Ugiliweneza, G. A. Hirsch, J. M. Wecht and S. Harkema (2021). "Restoration of autonomic cardiovascular regulation in spinal cord injury with epidural stimulation: a case series." Clin Auton Res **31**(2): 317-320.

Lewis, D. I. and J. H. Coote (1990). "The influence of 5-hydroxytryptamine agonists and antagonists on identified sympathetic preganglionic neurones in the rat, in vivo." Br J Pharmacol **99**(4): 667-672.

Liu, J. and L. M. Jordan (2005). "Stimulation of the parapyramidal region of the neonatal rat brain stem produces locomotor-like activity involving spinal 5-HT7 and 5-HT2A receptors." J Neurophysiol **94**(2): 1392-1404.

Llewellyn-Smith, I. J. and A. J. M. Verberne (2011). Central regulation of autonomic functions. New York, Oxford University Press.

Llinas, R. R. (1988). "The intrinsic electrophysiological properties of mammalian neurons: Insights into central nervous system function." Science **242**: 1654-1664.

Loewy, A. D. and K. M. Spyer (1990). Central Regulation of Autonomic Functions. Toronto, Ontario, Oxford University Press.

Logan, S. D., A. E. Pickering, I. C. Gibson, M. F. Nolan and D. Spanswick (1996). "Electrotonic coupling between rat sympathetic preganglionic neurones in vitro." J Physiol **495 (Pt 2)**: 491-502.

Luo, S., H. Xu, Y. Zuo, X. Liu and A. H. All (2020). "A Review of Functional Electrical Stimulation Treatment in Spinal Cord Injury." Neuromolecular Med **22**(4): 447-463.

Ma, R. C. and N. J. Dun (1985). "Norepinephrine depolarizes lateral horn cells of neonatal rat spinal cord in vitro." Neurosci Lett **60**(2): 163-168.

MacLean, J. N., K. C. Cowley and B. J. Schmidt (1998). "NMDA receptor-mediated oscillatory activity in the neonatal rat spinal cord is serotonin dependent." Journal of Neurophysiology **79**: 2804-2808.

Madden, C. J. and S. F. Morrison (2006). "Serotonin potentiates sympathetic responses evoked by spinal NMDA." J Physiol **577**(Pt 2): 525-537.

Magnuson, D. S. and T. C. Trinder (1997). "Locomotor rhythm evoked by ventrolateral funiculus stimulation in the neonatal rat spinal cord in vitro." J Neurophysiol **77**(1): 200-206.

Malpas, S. C. (1998). "The rhythmicity of sympathetic nerve activity." Prog Neurobiol **56**(1): 65-96.

Marder, E. and D. Bucher (2001). "Central pattern generators and the control of rhythmic movements." Curr Biol **11**(23): R986-996.

Marina, N., M. Taheri and M. P. Gilbey (2006). "Generation of a physiological sympathetic motor rhythm in the rat following spinal application of 5-HT." J Physiol **571**(Pt 2): 441-450.

Marks, S. A., R. D. Stein, M. R. Dashwood and M. P. Gilbey (1990). "[3H]prazosin binding in the intermediolateral cell column and the effects of iontophoresed methoxamine on sympathetic preganglionic neuronal activity in the anaesthetized cat and rat." Brain Res **530**(2): 321-324.

Maxwell, D. J., J. S. Riddell and E. Jankowska (2000). "Serotoninergic and noradrenergic axonal contacts associated with premotor interneurons in spinal pathways from group II muscle afferents." Eur J Neurosci **12**(4): 1271-1280.

McClellan, A. D. and S. Grillner (1984). "Activation of 'fictive swimming' by electrical microstimulation of brainstem locomotor regions in an in vitro preparation of the lamprey central nervous system." Brain Res **300**(2): 357-361.

McClellan, A. D., D. McPherson and M. J. O'Donovan (1994). "Combined retrograde labeling and calcium imaging in spinal cord and brainstem neurons of the lamprey." Brain Res **663**(1): 61-68.

McCrea, D. A. and I. A. Rybak (2008). "Organization of mammalian locomotor rhythm and pattern generation." Brain Res Rev **57**(1): 134-146.

McDonald, J. W. and C. Sadowsky (2002). "Spinal-cord injury." Lancet **359**(9304): 417-425.

Menelaou, E. and D. L. McLean (2012). "A gradient in endogenous rhythmicity and oscillatory drive matches recruitment order in an axial motor pool." J Neurosci **32**(32): 10925-10939.

Mneimneh, F., C. Moussalem, N. Ghaddar, K. Aboughali and I. Omeis (2019). "Influence of cervical spinal cord injury on thermoregulatory and cardiovascular responses in the human body: Literature review." J Clin Neurosci **69**: 7-14.

Mo, N. and N. J. Dun (1987). "Is glycine an inhibitory transmitter in rat lateral horn cells?" Brain Research **400**: 139-144.

Mori, S. (1987). "Integration of posture and locomotion in acute decerebrate cats and in awake, freely moving cats." Prog Neurobiol **28**(2): 161-195.

Müller-Jensen, L., C. J. Ploner, D. Kroneberg and W. U. Schmidt (2021). "Clinical Presentation and Causes of Non-traumatic Spinal Cord Injury: An Observational Study in Emergency Patients." Front Neurol **12**: 701927.

Muramoto, T., B. Mendelson, K. D. Phelan, E. Garcia-Rill, R. D. Skinner and C. Puskarich-May (1996). "Developmental changes in the effects of serotonin and N-methyl-D-aspartate on intrinsic membrane properties of embryonic chick motoneurons." Neuroscience **75**(2): 607-618.

Myers, J., M. Lee and J. Kiratli (2007). "Cardiovascular disease in spinal cord injury: an overview of prevalence, risk, evaluation, and management." Am J Phys Med Rehabil **86**(2): 142-152.

Nathan, P. W. and M. C. Smith (1987). "The location of descending fibres to sympathetic preganglionic vasomotor and sudomotor neurons in man." J Neurol Neurosurg Psychiatry **50**(10): 1253-1262.

Neuman, R. S. (1985). "Action of serotonin and norepinephrine on spinal motoneurones following blockade of synaptic transmission." Can J Physiol Pharmacol **63**(6): 735-738.

Newton, B. W., A. B. Burkhart and R. W. Hamill (1989). "Immunohistochemical distribution of serotonin in spinal autonomic nuclei: II. Early and late postnatal ontogeny in the rat." J Comp Neurol **279**(1): 82-103.

Nightingale, T. E., M. Walter, A. M. M. Williams, T. Lam and A. V. Krassioukov (2019). "Ergogenic effects of an epidural neuroprosthesis in one individual with spinal cord injury." Neurology **92**(7): 338-340.

Noga, B. R., D. J. Kriellaars and L. M. Jordan (1991). "The effect of selective brainstem or spinal cord lesions on treadmill locomotion evoked by stimulation of the mesencephalic or pontomedullary locomotor regions." Journal of Neuroscience **11(6)**: 1691-1700.

Noonan, V. K., M. Fingas, A. Farry, D. Baxter, A. Singh, M. G. Fehlings and M. F. Dvorak (2012). "Incidence and prevalence of spinal cord injury in Canada: a national perspective." Neuroepidemiology **38**(4): 219-226.

Noonan, V. K., B. K. Kwon, L. Soril, M. G. Fehlings, R. J. Hurlbert, A. Townson, M. Johnson, M. F. Dvorak and R. Network (2012). "The Rick Hansen Spinal Cord Injury Registry (RHSCIR): a national patient-registry." Spinal Cord **50**(1): 22-27.

Orer, H. S., M. E. Clement, S. M. Barman, S. Zhong, G. L. Gebber and R. B. McCall (1996). "Role of serotonergic neurons in the maintenance of the 10-Hz rhythm in sympathetic nerve discharge." Am J Physiol **270**(1 Pt 2): R174-181.

Paredes, R. M., J. C. Etzler, L. T. Watts, W. Zheng and J. D. Lechleiter (2008). "Chemical calcium indicators." Methods **46**(3): 143-151.

Parittotokkaporn, S., C. Varghese, G. O'Grady, D. Svirskis, S. Subramanian and S. J. O'Carroll (2020). "Non-invasive neuromodulation for bowel, bladder and sexual restoration following spinal cord injury: A systematic review." Clin Neurol Neurosurg **194**: 105822.

Peppler, W. T., W. J. Kim, K. Ethans and K. C. Cowley (2017). "Precision of dual-energy X-ray absorptiometry of the knee and heel: methodology and implications for research to reduce bone mineral loss after spinal cord injury." Spinal Cord **55**(5): 483-488.

Perreault, M. C., T. Drew and S. Rossignol (1993). "Activity of medullary reticulospinal neurons during fictive locomotion." J Neurophysiol **69**(6): 2232-2247.

Phillips, A. A. and A. V. Krassioukov (2015). "Contemporary Cardiovascular Concerns after Spinal Cord Injury: Mechanisms, Maladaptations, and Management." J Neurotrauma **32**(24): 1927-1942.

Phillips, A. A., J. W. Squair, D. G. Sayenko, V. R. Edgerton, Y. Gerasimenko and A. V. Krassioukov (2018). "An Autonomic Neuroprosthesis: Noninvasive Electrical Spinal Cord Stimulation Restores Autonomic Cardiovascular Function in Individuals with Spinal Cord Injury." J Neurotrauma **35**(3): 446-451.

Pickering, A. E., D. Spanswick and S. D. Logan (1994). "5-Hydoxytryptamine evokes depolarizations and membrane potential oscillations in rat sympathetic preganglionic neurones." J Physiol **480 (Pt 1)**(Pt 1): 109-121.

Pierce, M. L., J. Deuchars and S. A. Deuchars (2010). "Spontaneous Rhythmogenic Capabilities of Sympathetic Neuronal Assemblies in the Rat Spinal Cord Slice." Neuroscience **170**(3): 827-838.

Popa, C., F. Popa, V. T. Grigorean, G. Onose, A. M. Sandu, M. Popescu, G. Burnei, V. Strambu and C. Sinescu (2010). "Vascular dysfunctions following spinal cord injury." J Med Life **3**(3): 275-285.

Potter, P. J. (2006). "Disordered control of the urinary bladder after human spinal cord injury: what are the problems?" Prog Brain Res **152**: 51-57.

Rajaofetra, N., F. Sandillon, M. Geffard and A. Privat (1989). "Pre- and post-natal ontogeny of serotonergic projections to the rat spinal cord." J Neurosci Res **22**(3): 305-321.

Rancic, V., F. Haque, K. Ballanyi and S. Gosgnach (2019). "Using an upright preparation to identify and characterize locomotor related neurons across the transverse plane of the neonatal mouse spinal cord." J Neurosci Methods **323**: 90-97.

Rejc, E., C. Angeli and S. Harkema (2015). "Effects of Lumbosacral Spinal Cord Epidural Stimulation for Standing after Chronic Complete Paralysis in Humans." PLoS One **10**(7): e0133998.

Rekand, T., E. M. Hagen and M. Grønning (2012). "Chronic pain following spinal cord injury." Tidsskr Nor Laegeforen **132**(8): 974-979.

Rekand, T., E. M. Hagen and M. Grønning (2012). "Spasticity following spinal cord injury." Tidsskr Nor Laegeforen **132**(8): 970-973.

Roberts, T. T., G. R. Leonard and D. J. Cepela (2017). "Classifications In Brief: American Spinal Injury Association (ASIA) Impairment Scale." Clin Orthop Relat Res **475**(5): 1499-1504.

Rossignol, S. and A. Frigon (2011). "Recovery of locomotion after spinal cord injury: some facts and mechanisms." Annu Rev Neurosci **34**: 413-440.

Rousseau, V., R. Engelmann and B. A. Sabel (1999). "Restoration of vision III: soma swelling dynamics predicts neuronal death or survival after optic nerve crush in vivo." Neuroreport **10**(16): 3387-3391.

Rybak, I. A., N. A. Shevtsova, M. Lafreniere-Roula and D. A. McCrea (2006). "Modelling spinal circuitry involved in locomotor pattern generation: insights from deletions during fictive locomotion." J Physiol **577**(Pt 2): 617-639.

Sato, A. (1987). "Neural mechanisms of somatic sensory regulation of catecholamine secretion from the adrenal gland." Adv Biophys **23**: 39-80.

Sato, A. (1997). "Neural mechanisms of autonomic responses elicited by somatic sensory stimulation." Neurosci Behav Physiol **27**(5): 610-621.

Schmidt, B. J. and L. M. Jordan (2000). "The role of serotonin in reflex modulation and locomotor rhythm production in the mammalian spinal cord." Brain Res Bull **53**(5): 689-710.

Sharples, S. A., N. E. Burma, J. Borowska-Fielding, C. H. T. Kwok, S. E. A. Eaton, G. B. Baker, C. Jean-Xavier, Y. Zhang, T. Trang and P. J. Whelan (2020). "A dynamic role for dopamine receptors in the control of mammalian spinal networks." Sci Rep **10**(1): 16429.

Shik, M. L., F. V. Severin and G. N. Orlovsky (1969). "Control of walking and running by means of electrical stimulation of the mesencephalon." Electroencephalogr Clin Neurophysiol **26**(5): 549.

Singh, A., L. Tetreault, S. Kalsi-Ryan, A. Nouri and M. G. Fehlings (2014). "Global prevalence and incidence of traumatic spinal cord injury." Clin Epidemiol **6**: 309-331.

Sipski, M. L. (1991). "The impact of spinal cord injury on female sexuality, menstruation and pregnancy: a review of the literature." J Am Paraplegia Soc **14**(3): 122-126.

Smith, J. E., A. S. Jansen, M. P. Gilbey and A. D. Loewy (1998). "CNS cell groups projecting to sympathetic outflow of tail artery: neural circuits involved in heat loss in the rat." Brain Res **786**(1-2): 153-164.

Spanswick, D. and S. D. Logan (1990). "Spontaneous rhythmic activity in the intermediolateral cell nucleus of the neonate rat thoracolumbar spinal cord in vitro." Neuroscience **39(2)**: 395-403.

Spanswick, D., L. P. Renaud and S. D. Logan (1998). "Bilaterally evoked monosynaptic EPSPs, NMDA receptors and potentiation in rat sympathetic preganglionic neurones in vitro." J Physiol **509 (Pt 1)**(Pt 1): 195-209.

Squair, J. W., M. Gautier, L. Mahe, J. E. Soriano, A. Rowald, A. Bichat, N. Cho, M. A. Anderson, N. D. James, J. Gandar, A. V. Incognito, G. Schiavone, Z. K. Sarafis, A. Laskaratos, K. Bartholdi, R. Demesmaeker, S. Komi, C. Moerman, B. Vaseghi, B. Scott, R. Rosentreter, C. Kathe, J. Ravier, L. McCracken, X. Kang, N. Vachicouras, F. Fallegger, I. Jelescu, Y. Cheng, Q. Li, R. Buschman, N. Buse, T. Denison, S. Dukelow, R. Charbonneau, I. Rigby, S. K. Boyd, P. J. Millar, E. M. Moraud, M. Capogrosso, F. B. Wagner, Q. Barraud, E. Bezard, S. P. Lacour, J. Bloch, G. Courtine and A. A. Phillips (2021).

"Neuroprosthetic baroreflex controls haemodynamics after spinal cord injury." Nature **590**(7845): 308-314.

Steeves, J. D. and L. M. Jordan (1980). "Localization of a descending pathway in the spinal cord which is necessary for controlled treadmill locomotion." Neuroscience Letters **20**: 283-288.

Stiens, S. A., S. B. Bergman and L. L. Goetz (1997). "Neurogenic bowel dysfunction after spinal cord injury: clinical evaluation and rehabilitative management." Arch Phys Med Rehabil **78**(3 Suppl): S86-102.

Strack, A. M., W. B. Sawyer, L. M. Marubio and A. D. Loewy (1988). "Spinal origin of sympathetic preganglionic neurons in the rat." Brain Res **455**(1): 187-191.

Stuart, D. G. and H. Hultborn (2008). "Thomas Graham Brown (1882--1965), Anders Lundberg (1920-), and the neural control of stepping." Brain Res Rev **59**(1): 74-95.

Szokol, K., J. C. Glover and M. C. Perreault (2011). "Organization of functional synaptic connections between medullary reticulospinal neurons and lumbar descending commissural interneurons in the neonatal mouse." J Neurosci **31**(12): 4731-4742.

Szokol, K. and M. C. Perreault (2009). "Imaging synaptically mediated responses produced by brainstem inputs onto identified spinal neurons in the neonatal mouse." J Neurosci Methods **180**(1): 1-8.

Tada, M., A. Takeuchi, M. Hashizume, K. Kitamura and M. Kano (2014). "A highly sensitive fluorescent indicator dye for calcium imaging of neural activity in vitro and in vivo." Eur J Neurosci **39**(11): 1720-1728.

Takahashi, T. and A. J. Berger (1990). "Direct excitation of rat spinal motoneurones by serotonin." Journal of Physiology **423**: 63-76.

Tang, X., N. D. Neckel and L. P. Schramm (2004). "Spinal interneurons infected by renal injection of pseudorabies virus in the rat." Brain Res **1004**(1-2): 1-7.

van den Brand, R., J. Heutschi, Q. Barraud, J. DiGiovanna, K. Bartholdi, M. Huerlimann, L. Friedli, I. Vollenweider, E. M. Moraud, S. Duis, N. Dominici, S. Micera, P. Musienko and G. Courtine (2012). "Restoring voluntary control of locomotion after paralyzing spinal cord injury." Science **336**(6085): 1182-1185.

Viala, D. and C. Vidal (1978). "Evidence for distinct spinal locomotion generators supplying respectively fore- and hindlimbs in the rabbit." Brain Res **155**(1): 182-186.

Wang, L. H., E. Spary, J. Deuchars and S. A. Deuchars (2008). "Tonic GABAergic Inhibition of Sympathetic Preganglionic Neurons: A Novel Substrate for Sympathetic Control." Journal of Neuroscience **28**(47): 12445-12452.

Wang, M. Y. and N. J. Dun (1990). "5-Hydroxytryptamine responses in neonate rat motoneurones in vitro." Journal of Physiology **430**: 87-103.

Weaver, L. C., J. C. Fleming, C. J. Mathias and A. V. Krassioukov (2012). "Disordered cardiovascular control after spinal cord injury." Handb Clin Neurol **109**: 213-233.

Wecht, J. M., A. V. Krassioukov, M. Alexander, J. P. Handrakis, S. L. McKenna, M. Kennelly, M. Trbovich, F. Biering-Sorensen, S. Burns, S. L. Elliott, D. Graves, J. Hamer, K. Krogh, T. A. Linsenmeyer, N. Liu, E. M. Hagen, A. A. Phillips, J. G. Previnaire, G. M. Rodriguez, C. Slocum and J. R. Wilson (2021). "International Standards to document Autonomic Function following SCI (ISAFSCI): Second Edition." Top Spinal Cord Inj Rehabil **27**(2): 23-49.

Wen, H., Y. Chen, Y. He, C. S. Bickel, S. Robinson-Whelen and A. W. Heinemann (2018). "Racial Differences in Weight Gain: A 5-Year Longitudinal Study of Persons With Spinal Cord Injury." Arch Phys Med Rehabil **99**(10): 1957-1964.

Whelan, P., A. Bonnot and M. J. O'Donovan (2000). "Properties of rhythmic activity generated by the isolated spinal cord of the neonatal mouse." **84**(6): 2821-2833.

Whelan, P. J. (1996). "Control of locomotion in the decerebrate cat." Prog Neurobiol **49**(5): 481-515.

Williams, R. and A. Murray (2015). "Prevalence of depression after spinal cord injury: a meta-analysis." Arch Phys Med Rehabil **96**(1): 133-140.

World Health Organization. (2013, 19 November). "Spinal Cord Injury." Retrieved December 11, 2019, from https://www.who.int/news-room/fact-sheets/detail/spinal-cord-injury.

Zaporozhets, E., K. C. Cowley and B. J. Schmidt (2004). "A reliable technique for the induction of locomotor-like activity in the in vitro neonatal rat spinal cord using brainstem electrical stimulation." J Neurosci Methods **139**(1): 33-41.

Zaporozhets, E., K. C. Cowley and B. J. Schmidt (2006). "Propriospinal neurons contribute to bulbospinal transmission of the locomotor command signal in the neonatal rat spinal cord." J Physiol **572**(Pt 2): 443-458.

Zhang, H., N. A. Shevtsova, D. Deska-Gauthier, C. Mackay, K. J. Dougherty, S. M. Danner, Y. Zhang and I. A. Rybak (2022). "The role of V3 neurons in speed-dependent interlimb coordination during locomotion in mice." Elife **11**.

Zong, W., H. A. Obenhaus, E. R. Skytøen, H. Eneqvist, N. L. de Jong, R. Vale, M. R. Jorge, M. B. Moser and E. I. Moser (2022). "Large-scale two-photon calcium imaging in freely moving mice." Cell **185**(7): 1240-1256.e1230.